REVIEW

Check for updates

An overview of metamaterials and their achievements in wireless power transfer

Kai Sun,[abc] Runhua Fan,*[a] Xihua Zhang,[b] Zidong Zhang,[b] Zhicheng Shi, [ID][d] Ning Wang,*[e] Peitao Xie,[b] Zhongyang Wang,[b] Guohua Fan,[b] Hu Liu, [ID][f] Chuntai Liu,*[f] Tingxi Li,[g] Chao Yan [ID][h] and Zhanhu Guo [ID]*[c]

Metamaterials have been deployed for a wide range of fields including invisible cloak, superlens, electromagnetic wave absorption and magnetic resonance imaging, owing to their peculiar electromagnetic properties. However, few investigations on metamaterials were focused on wireless power transfer (WPT). WPT is the transmission of electrical energy from a power source to an electrical load without conductors like wires or cables. Metamaterials can enhance the transfer efficiency and enlarge the transfer distance due to their ability of focusing magnetic flux, which opens up a novel approach to promoting the development and application of WPT. This review paper aims to provide an overview of the fabrications, exotic properties, and their applications especially in the WPT field. Meanwhile, the perspective and future challenges of metamaterials and WPT are proposed.

[a] College of Ocean Science and Engineering, Shanghai Maritime University, Shanghai 201306, China. E-mail: rhfan@shmtu.edu.cn

[b] Key Laboratory for Liquid-Solid Structural Evolution and Processing of Materials (Ministry of Education), Shandong University, Jinan, 250061, China

[c] Integrated Composites Laboratory (ICL), Department of Chemical & Biomolecular Engineering, University of Tennessee, Knoxville, TN 37996, USA. E-mail: zguo10@utk.edu

[d] Institute of Material Science and Engineering, Ocean University of China, Qingdao, 266100, China

[e] State Key Laboratory of Electronic Thin Film and Integrated Devices, University of Electronic Science and Technology of China, Chengdu 610054, China

[f] National Engineering and Research Center for Advanced Polymer Processing Technology, Zhengzhou University, Zhengzhou, 450001, China

[g] College of Materials Science and Engineering, Shandong University of Science and Technology, Qingdao, 266590, China

[h] School of Material Science and Engineering, Jiangsu University of Science and Technology, Zhenjiang, Jiangsu, China

Dr Kai Sun, currently an Assistant Professor at the College of Ocean Science and Engineering, Shanghai Maritime University, Shanghai, China, obtained his PhD degree in Material Science and Engineering from Shandong University (2017). During his graduate study, he worked as a joint Material Science and Engineering PhD student at the University of Tennessee sponsored by the China Scholarship Council (CSC). His current research mainly focuses on the preparation process, structure design and performance control of metamaterials, energy storage and electronic devices.

Kai Sun

Dr Runhua Fan, currently a Professor at the College of Ocean Science and Engineering, Shanghai Maritime University (SMU), Shanghai, China, obtained a PhD degree in Shandong University (2001). Dr Fan was the vice-chair of the Key Laboratory for Liquid–Solid Structural Evolution and Processing of Materials (Ministry of Education), and serves as the deputy director of the College of Ocean Science and Engineering in SMU. His current research interests focus on the structure/function integrating of multifunctional composites, electromagnetic wave shielding/absorption, electronic devices and energy storage.

Runhua Fan

1. Introduction

Metamaterials are artificial materials composed of periodic structure units to gain their unusual properties, which are not found in nature.[1] Generally, metamaterials obtain their peculiar properties from their structural arrays rather than compositions and microstructures. According to different physical properties, metamaterials can be classified into acoustic, thermal, photonic and electromagnetic (EM) metamaterials, *etc.* Recently, EM metamaterials, which are constructed by subwavelength structure units, have been paid extensive attention due to their exotic properties, such as reversed Doppler effect,[2] reversed Vavilov-Cherenkov radiation,[3] negative refraction index,[1] double negative property,[4] *etc.* EM metamaterials simultaneously possess negative permittivity and negative permeability (*i.e.*, $\varepsilon < 0$ and $\mu < 0$),

and obey the left-handed rule, which are different from conventional materials. Hence, EM metamaterials are also termed as double negative materials or left-handed materials due to their exotic electromagnetic property.

Actually, it took a long time to realize the negative permittivity and negative permeability behavior in artificial EM metamaterials from theory to practice. In 1968, Veselago[5] initially made a theoretical study and proposed the hypothesis of double negative materials. However, in the following several decades, there was no significant progress in double negative materials due to science and technology limitations. At the end of the 1990s, Pendry[6] theoretically proved the feasibility to realize negative refraction and constructed a "perfect lens" with a negative refraction index $n = -1$ (*i.e.*, $\varepsilon = -1$ and $\mu = -1$), beyond the diffraction limit. Based on Pendry's theoretical investigation, Smith *et al.*[7]
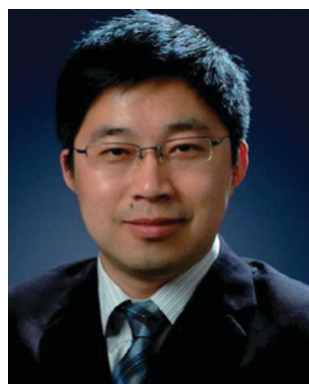
Dr Zidong Zhang, currently an Associate Professor at the School of Material Science and Engineering, Shandong University, Jinan, China, obtained a PhD degree in Material Science and Engineering from Shandong University (2013). He worked as a visiting scholar (2012–2013) in the Institute for Superconducting and Electronic Materials (ISEM), University of Wollongong, Australia. His current research focuses on metamaterials, electromagnetic nanocomposites, and electronic devices.

Zidong Zhang

Dr Zhicheng Shi, currently an Associate Professor at the Institute of Material Science and Engineering, Ocean University of China, Qingdao, China, obtained a PhD degree in Material Science and Engineering from Shandong University (2013). He has worked as a visiting scholar at the Georgia Institute of Technology from 2017. His current research focuses on metamaterials, multifunctional composites especially magnetic and conductive materials, and advanced dielectric materials.

Zhicheng Shi

Dr Ning Wang, currently a Professor at State Key Laboratory of Electronic Thin Film and Integrated Devices, University of Electronic Science and Technology of China, obtained a PhD degree in Materials Science and Engineering from Tsinghua University, China (2007) and received two-year (2008–2010) postdoctoral training at the Department of Applied Chemistry at Nagoya University, Japan. His current research focuses on the fundamental science of nanomaterials applied in energy-related materials and devices.

Ning Wang

Dr Hu Liu is currently an associate professor at Zhengzhou University. He obtained his PhD from Zhengzhou University (2017), and worked as a joint PhD student with Prof. Zhanhu Guo at the University of Tennessee, sponsored by the China Scholarship Council (CSC). His current research interest focuses on flexible conductive polymer composites for strain sensors, electromagnetic radiation shielding and polymer processing-microstructure-properties. Dr Hu Liu is currently an associate professor at Zhengzhou University. He obtained his PhD from Zhengzhou University (2017), and worked as a joint PhD student with Prof. Zhanhu Guo at the University of Tennessee, sponsored by the China Scholarship Council (CSC). His current research interest focuses on flexible conductive polymer composites for strain sensors, electromagnetic radiation shielding and polymer processing-microstructure-properties.

Hu Liu

2926 | *J. Mater. Chem. C,* 2018, **6**, 2925–2943

This journal is © The Royal Society of Chemistry 2018

experimentally achieved negative permeability and negative permittivity in microwave frequencies in 2001, *via* artificially fabricating EM metamaterials with periodic split ring resonators (SRR) and copper wires. It was demonstrated that the negative permeability was attributed to the *LC* resonance produced by the SRR, and the negative permittivity resulted from the conductive copper wires. Since then, the number of investigations about EM metamaterials has rapidly grown and extended to microwave,[8–10] infrared[11–13] and visible frequency regions.[14–16] Meanwhile, various EM metamaterials were fabricated, in which the periodic unit cell possessed different dimensions and structures.[17–20] In a narrow sense, an EM metamaterial is an arrangement of artificial structure units designed to achieve unusual electromagnetic properties, which cannot be observed in natural materials. However, in a broad sense, an EM metamaterial is not only a novel material with unique properties, but also an innovative design concept of fabricating advanced materials with tunable properties.

In recent years, increasing investigations based on metamaterials have been focused on energy harvesting,[21,22] invisible cloak,[23,24] superlens,[1,25] and magnetic resonance imaging[26,27] owing to their peculiar electromagnetic properties. However, less attention was paid to wireless power transfer (WPT) applications based on metamaterials in previous reviews.[28–31] WPT is the transmission of electrical energy from a power source to an electrical load without conductors like wires or cables.[32] Compared with traditional power transfer forms,[33] WPT can improve the safety, reliability and lifespan of the power supply system[34,35] and possesses significant applications in the field of electric vehicles,[36] lighting,[37] implantable medical devices[38] and mobile phone charging,[39] *etc.* In fact, there are urgent requirements for WPT to improve the transfer efficiency and distance, which play a primary role in its development and practical applications. This indicates that EM metamaterials can significantly enhance transfer efficiency and have great potential applications in the energy transmission field due to their unique properties,[40] which will open up a novel approach to promote the development and application of WPT. It is worth noting that fewer reviews about metamaterials focused on their applications in the WPT field. On the other hand, in the reviews on WPT science and technology,[34,41–43] the current work is mainly concentrated on the configuration design rather than materials. Therefore, this review paper provides an overview of the chemical synthesis, exotic properties, and past achievements of EM metamaterials as well as their applications, especially in the WPT field. Meanwhile, the perspective and future challenges of metamaterials and WPT are proposed. For the sake of convenience, electromagnetic metamaterials are abbreviated to metamaterials in the following sections.

2. Electromagnetic properties of metamaterials

Permittivity and permeability are two constitutive parameters characterizing the electromagnetic properties of materials.[44,45] According to different values of permittivity and permeability, materials can be classified into four categories (Fig. 1). For conventional materials, the permittivity and permeability are both positive. When either permittivity or permeability is negative (*i.e.*, $\varepsilon < 0$, $\mu > 0$ or $\varepsilon > 0$, $\mu < 0$), the materials are called epsilon-negative (*e.g.*, metals,[46] plasmas[47]) or mu-negative materials (*e.g.*, gyrotropic magnetic materials[48]). Interestingly, when these two parameters are simultaneously negative, materials are defined as double negative materials. In fact, the double negative property was initially observed in metamaterials. When the values of ε and μ are simultaneously positive or negative, the electromagnetic waves can propagate through the media. For the conventional materials ($\varepsilon > 0$, $\mu > 0$), the electric vector **E**, magnetic vector **H** and wave vector **K** correspond

Dr Chuntai Liu, currently a Professor of the National Engineering Research Center for Advanced Polymer Processing Technology (NERC) of Zhengzhou University, obtained his PhD from Zhengzhou University (2003), and worked as a visiting scholar at the Ohio State University (2006–2007). He serves as the deputy director of NERC of Zhengzhou University. His research focuses on multifunctional polymer composites including processing-microstructure-properties.

Chuntai Liu

Dr Zhanhu Guo, an Associate Professor in the Department of Chemical and Biomolecular Engineering, University of Tennessee, Knoxville, USA, obtained a PhD degree in Chemical Engineering from Louisiana State University (2005) and received three-year (2005–2008) postdoctoral training from the Mechanical and Aerospace Engineering Department at the University of California Los Angeles. Dr Guo chaired the Composite Division of the American Institute of Chemical Engineers (AIChE, 2010–2011) and directs the Integrated Composites Laboratory. His current research focuses on multifunctional nanocomposites for education, transportation, safety, information, catalysis, energy harvesting and storage, electronics and environmental remediation applications.
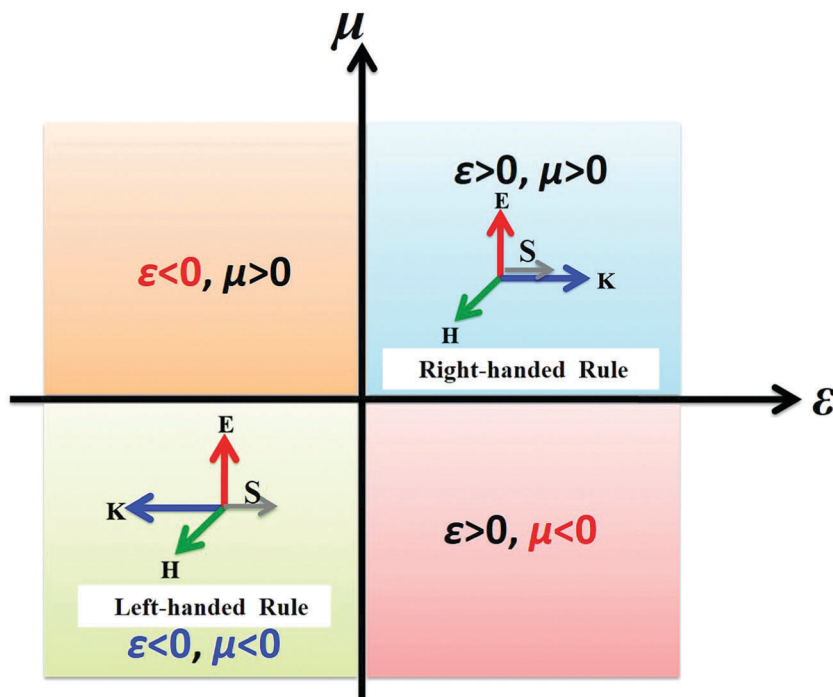
Zhanhu Guo

Fig. 1 The categories of materials based on different permittivity (ε) and permeability (μ) values. The insets show the right/left-handed rules. *E*, *H*, *K*, and *S* are the electric field, magnetic field, wave propagation and Poynting vectors, respectively.

to the right-handed rule. Meanwhile, the Poynting vector *S*, representing energy flux density, has the same direction of wave propagation, which means the energy decays along with the propagation.

For metamaterials with a double negative property ($\varepsilon < 0$, $\mu < 0$), the electromagnetic waves can propagate through the media and satisfy the Maxwell equations, eqn (1)–(4),[49]

$$\boldsymbol{k} \times \boldsymbol{E} = \omega\mu\boldsymbol{H} \tag{1}$$

$$\boldsymbol{k} \times \boldsymbol{H} = -\omega\varepsilon\boldsymbol{E} \tag{2}$$

$$\boldsymbol{k}\cdot\boldsymbol{E} = 0 \tag{3}$$

$$\boldsymbol{k}\cdot\boldsymbol{H} = 0 \tag{4}$$

When permittivity and permeability are both negative, the three vectors *E*, *H* and *K* of double negative materials obey the left-handed rule[3] and the Poynting vector is opposite to the wave vector direction, which is toward the source. In this case, it is demonstrated that the energy flow of the electromagnetic waves is opposite to the positive phase direction of the source. Hence, metamaterials can also be called backward-wave behavior.[49] An additionally significant property for metamaterials with double negative electromagnetic parameters is their negative refraction index character. As discussed above, the double negative property does not violate any fundamental laws; therefore, according to Snell's law,

$$n_1 \sin\theta_1 = n_2 \sin\theta_2 \tag{5}$$

where n_1, n_2, θ_1 and θ_2 are the refractive index of medium 1 and 2, the incident and refractive angles, respectively. For metamaterials

with negative permittivity and negative permeability, the incident beam and the refractive beam are on the same side of the normal. This indicates that the refractive index of metamaterials is a negative value, namely, $n = -\sqrt{\varepsilon\mu}$. In addition, metamaterials possess other unique properties, including a reversed Doppler effect, reversed Vavilov–Cherenkov radiation and reversed Goos–Hanchen shift, which are derived from these significant electromagnetic properties. According to their peculiar electromagnetic properties, metamaterials have great potential applications in the field of invisible cloak, superlens, electromagnetic wave absorption and microstrip antennas,[50] *etc.* In recent years, it was reported that metamaterials with negative permeability can improve the resolution of magnetic resonance imaging due to their ability of focusing the radio-frequency magnetic field lines of force.[26] Additionally, the unique properties of metamaterials, especially evanescent wave amplification,[33] are of great significance to WPT because the resonant coupling is essentially the coupling of evanescent waves.[51] When a metamaterial is placed between the transmitter and receiver coils, the evanescent wave can be enhanced and the coupling coefficient can be improved as well, which leads to the increase of transfer efficiency and transfer distance. In the following, the mechanisms of negative permittivity and negative permeability behaviors are further explored and revealed.

Smith *et al.*[7] firstly fabricated metamaterials with periodic building blocks and experimentally observed negative refraction index in the microwave frequency region (Fig. 2). The copper split ring resonators (SRR) and copper wires were distributed on both sides of insulating Teflon substrate *via* shadow mask/ etching technique. Subsequently, the individual structure units
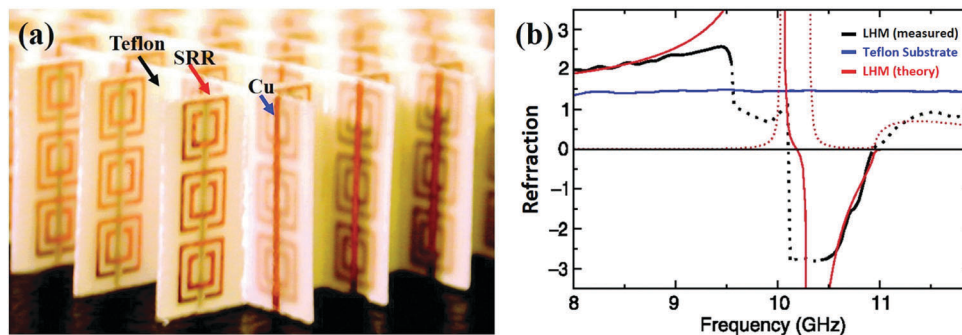
Fig. 2 Realization of negative refraction derived from metamaterials.[7] (a) The periodic structure of metamaterials and (b) the negative refraction of metamaterials. Redrawn from ref. 7.

were assembled into resulting metamaterials, as shown in Fig. 2a. Compared with pristine Teflon, these metamaterials with a conductive copper component realized a negative refraction index by taking advantage of periodic structure arrays. Eqn (6) and (7) are the generic forms of the effective permittivity and permeability for metamaterials with periodic arrays,[7,52]

$$\varepsilon = \varepsilon_0 \left(1 - \frac{\omega_{pe}^2 - \omega_{0e}^2}{\omega^2 - \omega_{0e}^2 + i\omega\gamma_e}\right) \qquad (6)$$

$$\mu = \mu_0 \left(1 - \frac{\omega_{pm}^2 - \omega_{0m}^2}{\omega^2 - \omega_{0m}^2 + i\omega\gamma_m}\right) \qquad (7)$$

where ω_{0e} and ω_{0m} are the electronic and magnetic resonance frequencies, ω_{pe} and ω_{pm} are the electronic and magnetic plasma frequencies, γ_e and γ_m are the damping terms representing electric and magnetic dissipation, respectively. When the conductive wires in metamaterials cannot maintain electrical continuity, ω_{0e} is large than 0. When the wires establish a conductive network, it is in good accordance with the Drude model,[53] which is expressed as eqn (8)

$$\varepsilon = \varepsilon_0 \left(1 - \frac{\omega_{pe}^2}{\omega^2 + i\omega\gamma_e}\right) \qquad (8)$$

It was demonstrated that the negative permittivity behavior is attributable to the plasma collective oscillation of the electrons from metal. Below the plasma frequency, the dielectric constants of metals present negative values. In general, the plasma frequency of bulk metals is usually located in the ultraviolet or visible regions, which suggests that the absolute values of negative permittivity in bulk metals are too enormous and limit the practical applications. Hence, this requires us to obtain a weak negative permittivity and match the permeability. When the metal wires were periodically embedded in the matrix, the average concentration of electrons was diluted and the effective electron mass was enhanced due to self-inductance.[53] Therefore, the plasma frequency of metamaterials with thin metal wires can be reduced to the far infrared or even GHz band.[54] In addition, the negative permittivity can be adjusted by applying an external electric or thermal field.[55,56]

For metamaterials, the negative permeability was attributed to *LC* resonance[57] or Mie resonance derived from periodic structure.[58] When the structure units are composed of metal wires and SSR, the resultant metamaterials can be equivalent to a circuit including capacitance *C* and inductance *L*. This indicates that inductance comes from the metal wires. In addition, the splits can provide the capacitance. When the frequency of an electromagnetic wave equals the nature oscillation frequency of the metamaterials, the *LC* resonance occurs and gives rise to a negative permeability behavior. As a substitute for metamaterials with a metallic component, dielectric metamaterials were fabricated to decrease the energy loss. It was demonstrated that the Mie resonance leads to a negative permeability in the dielectric metamaterials.[59] When the electromagnetic wave frequency is close to the bandgap frequency of materials, it can excite the magnetic and electric dipole resonances due to the first Mie resonance and the second Mie resonance, respectively. These Mie resonances are accompanied by a characteristic resonant dispersion in the linear response regime, and thus an ensemble of spheres or an array of discs or cubes (metasurface) can be described by an effective negative dielectric permittivity at the electric resonance and by an effective negative magnetic permeability at the magnetic resonance.[31] It is suggested that the frequency dispersion of permeability in the radio frequency region corresponds to the domain wall resonance, and the gyromagnetic spin resonance plays an important role in the high frequency regime.[60] Tsutaoka *et al.* observed a negative permeability in ferrite materials, which was ascribed to the combined effects of domain-wall resonance and nature resonance.[61] Similarly, a negative permeability can also be controlled under the action of an external electromagnetic field.

3. Progress and fabrications of metamaterials

Since metamaterials with negative permittivity and negative permeability were fabricated, the metamaterial structure unit has changed from the initial square-shape to U-shape,[62] S-shape,[63] Ω-shape[64] and fishnet shape forms,[65] *etc.* Moreover, the size of the structure unit has changed from a millimeter-sized dimension to micro- and nano-sized dimensions. Meanwhile, the applied frequency range of metamaterials extended to the terahertz, infrared and visible frequency regions.[11,66,67] Afterwards, 2D metamaterials were also fabricated, which are called metasurfaces. Recently, flexible and stretchable

metamaterials draw more attention due to their promising applications in the field of wearable cloaks, sensing and flexible electronic devices.[68] For a typical metamaterial, the ratio of operating wavelength to unit cell size λ/a is usually more than 10, and thereby metamaterials can be regarded as effective media. Generally, the size of the structure unit for metamaterials depends on practical applications as well as the synthesis and fabrication methods. In the microwave frequency region, metamaterials are mainly fabricated by a shadow mask lithography method,[7,69] while in the terahertz or visible frequency region, metamaterials can be achieved by electron or ion beam lithography and laser direct writing techniques.[11,70–72] Moreover, 3D printing,[73] template deposition[74] and self-assembly[75] chemical techniques can attain metamaterials.

Fig. 3 shows the metamaterials with different dimensions and structures. Linden et al.[57] employed a nanofabrication technique to achieve metamaterials composed of U-shape nanosized gold unit cells (Fig. 3a). Compared with previous double split ring resonators, this array of single nonmagnetic gold split rings can also generate a magnetic resonance and attain a negative refraction index near 100 THz, which results from the inductor-capacitor circuit resonance. The effect of structure units' orientation on their electromagnetic property was also investigated, which indicated that metamaterials possess anisotropic characteristic. Dolling et al.[18] used an electron-beam lithography process to fabricate sandwich structural Ag–MgF$_2$–Ag metamaterials, which were located on a glass substrate coated with a 5 nm thin film of indium tin oxide to avoid the charging effects in the lithography process. As shown in Fig. 3b, the structure unit presented a nanosized fishnet shape, and the negative refraction index was observed at almost 780 nm wavelength in the silver-based metamaterials. A copper-based metamaterial was prepared via a shadow mask lithography method,[76] and the microsized structure units were

composed of circular split ring resonators (SRR) and copper wires (Fig. 3c), which exhibited negative permittivity and negative permeability in the microwave regime. Fan et al.[77] proposed a facile multilayer electroplating method to synthesize non-planar copper-based SRR on a flexible silicon substrate (Fig. 3d). The gap size and the total height of the SRR are determined by the thickness of the photoresist which can be tuned by the spinning rate. The negative permittivity behavior was observed owing to the plasma oscillation of copper electrons, and the negative permeability arose from LC resonance. The negative refraction index was attained in the terahertz frequency region. In addition, metamaterials with spiral and L-shaped structure units were prepared via nanofabrication methods (Fig. 3e and f).[78,79]

At present, the commonly flexible substrates for metamaterials are polydimethylsiloxane (PDMS),[80] polyethylene terephthalate (PET)[81] and polyimide (PI),[82] due to their suitable intrinsic properties, such as proper flexibility, lower dielectric constant and loss. Zhu et al.[83] employed shadow mask lithography and nanoprinting transfer processes to fabricate a flexible PDMS-based metamaterial membrane. Fig. 4a shows the preparation schematic for a high-contrast metastructure (HCM). Firstly, the silicon on insulator (SOI) wafer was treated by a thermal oxidation to precisely control the HCM thickness. Subsequently, the pattern was etched on the resist via ultraviolet lithography; then, the pattern on the resist was totally transferred to the SiO$_2$ hard mask by oxide dry etching. After treatment with hydrofluoric acid, the HCM structure was released. In the following preparation step, a PDMS stamp-based process was used to pick up the HCM from the SOI substrate via a nanoprinting transfer process. Finally, the HCMs on the stamp were encapsulated by a thin PDM layer by repeating the PDMS stamp preparation process. Top and cross-section SEM images of the HCM on SOI after
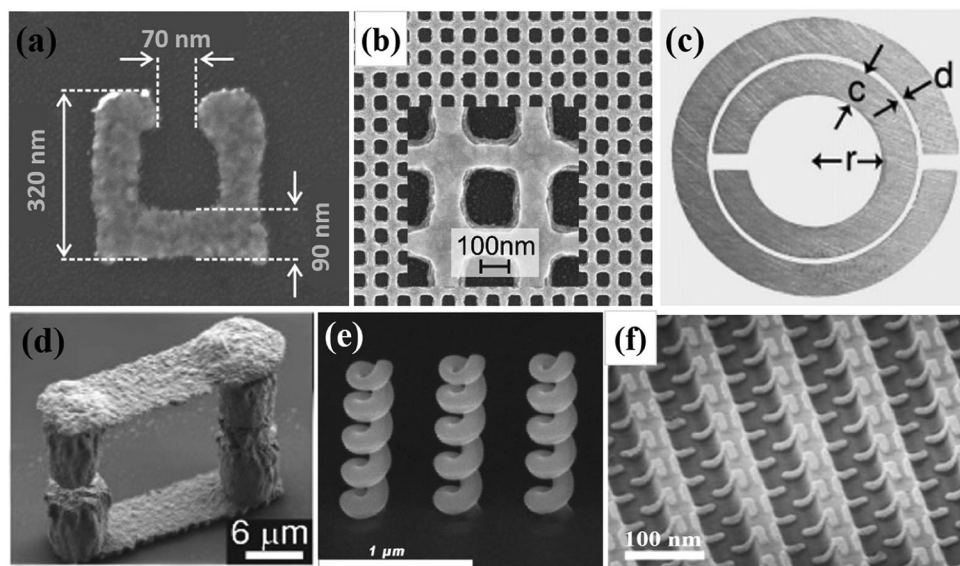

Fig. 3 Metamaterials with different dimensions and structures. (a–f) Are metamaterials with a nanosized U-shape,[57] nanosized fishnet,[18] millimeter-sized circle-shape,[76] flexible metamaterial with microsized U-shape structure,[77] nanosized spiral[79] and nanosized L-shape,[78] respectively. Redrawn from ref. 18 and 57. Reproduced with permission from ref. 76 and 77 (Open Access), ref. 78 and 79. Copyright (2000) American Physical Society, (2011) Optical Society of America, (2012) John Wiley and Sons and (2014) John Wiley and Sons.
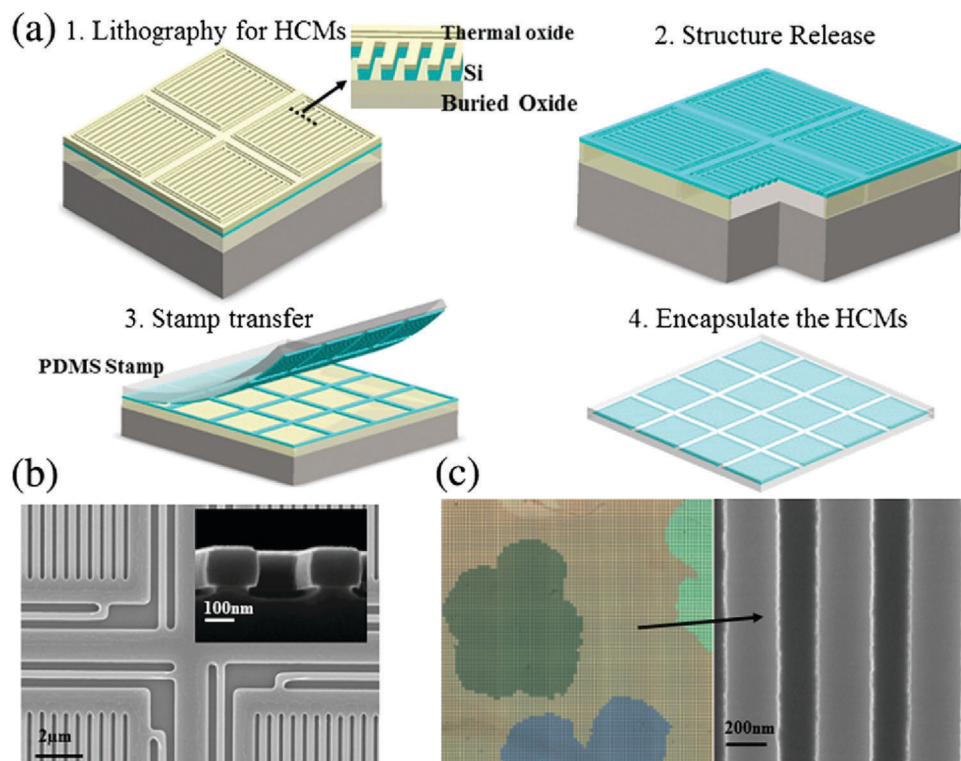
2930 | J. Mater. Chem. C, 2018, 6, 2925–2943

This journal is © The Royal Society of Chemistry 2018

Fig. 4 Flexible photonic metastructures.[83] (a) is the preparation schematic for a high-contrast metastructure (HCM). (b) are SEM images for a HCM on silicon on an insulator after etching. The inset shows the cross-section. (c) Microscopic (left) and SEM (right) images for the transferred HCMs on PDMS before encapsulation. The left image is a large 1 cm × 1 cm sample. Each individual pixel is 100 μm × 100 μm in size. The right image is the top view SEM of the HCM. Reproduced with permission from ref. 83 (Open Access). Copyright (2015) Optical Society of America.

etching are exhibited in Fig. 4b. The resulting metamaterial sample and microscopic images are shown in Fig. 4c. This technique opens a novel approach to metamaterial membranes, which can be applied in flexible optical devices. Additionally, other advanced fabrication methods, such as soft lithography,[84] interference lithography,[85] imprint lithography,[86] electroplating,[87] laser micro-lens array lithography[88] and microstereolithography,[89] have also been used to fabricate flexible metamaterials.

Recently, a different approach to metamaterials based on dielectric media instead of metal components has emerged. According to different practical applications, dielectric metamaterials can be divided into negative refraction index nano-resonators, metasurfaces, zero-index metamaterials, anisotropic metamaterials,[31] etc. The dielectric metamaterials with different structural units are shown in Fig. 5. Zhou et al.[58] prepared millimeter-sized $Ba_{0.5}Sr_{0.5}TiO_3$ bulks by tape-casting and pressureless sintering processes, and then the ceramic-based structure units were periodically embedded in a Teflon matrix (Fig. 5a). For $Ba_{0.5}Sr_{0.5}TiO_3$ dielectric metamaterials, the negative permeability behavior was attributed to the Mie resonance of the materials rather than LC resonance. It is worth noting that the negative refraction index observed in this ceramic-based metamaterial was in the frequency range of 7.5–9.0 GHz. Fan et al.[90] proposed a developed nano-solid-fluid assembly method to fabricate 3D all-dielectric metamaterial composed of 15 nm TiO_2 nanoparticles. This TiO_2-based metamaterial produced an
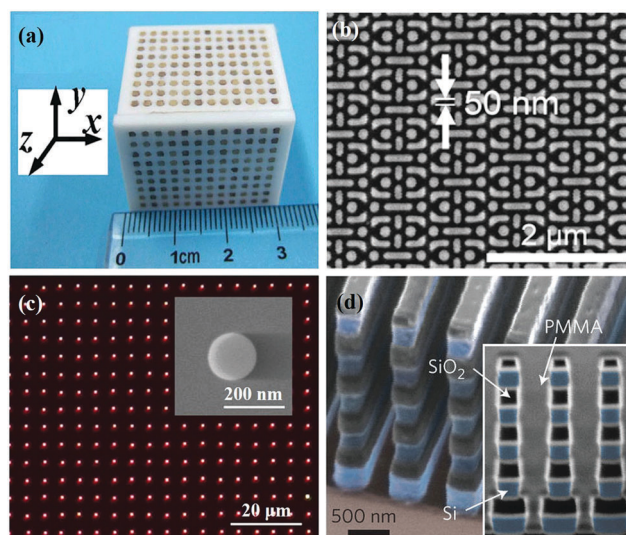

Fig. 5 Dielectric metamaterials with different structural units. (a–d) are $Ba_{0.5}Sr_{0.5}TiO_3$,[58] TiO_2,[90] silicon[91] and Si/SiO$_2$ dielectric metamaterials,[92] respectively. Redrawn from ref. 90. Reproduced with permission from ref. 58, 91 and 92. Copyright (2008) American Physical Society, (2014) Springer Nature and (2013) Springer Nature.

image with a super-resolution of 45 nm, which exceeded the traditional diffraction limit and could be promising in low-loss nanophotonic devices. Zywietz et al. fabricated a dielectric

This journal is © The Royal Society of Chemistry 2018

J. Mater. Chem. C, 2018, 6, 2925–2943 | 2931

metamaterial with submicron-sized silicon particles by a novel femtosecond laser pulses technique, which was based on laser-induced transfer of molten nanodroplets initiated by tightly focused laser pulses.[91] The Mie resonance was observed in optical frequency due to the strong electric and magnetic dipole responses from the silicon particles. This indicates that the silicon metamaterial could be a promising candidate for photonic crystals and nanoantenna. Moitra et al.[92] achieved multilayers Si/SiO_2 metamaterial using low-pressure chemical vapor deposition and reactive ion etching techniques. Poly(methyl methacrylate), i.e., PMMA, was spin-coated onto the sample to fill the air gaps. This demonstrates that the Si/SiO_2 metamaterial possesses an impedance-matched zero-index at optical frequencies, which could be applied in the field of directional light sources, angularly selective optical filters and large-area single-mode photonic devices.

Actually, there also exist random metamaterials apart from for periodic metamaterials. For example, Chui et al.[45] initially proposed the possibility of realizing a double negative property in random metallic magnetic granular composites based on the effective medium theory. The electromagnetic properties of metamaterials with randomly disordered structures are shown in Fig. 6.
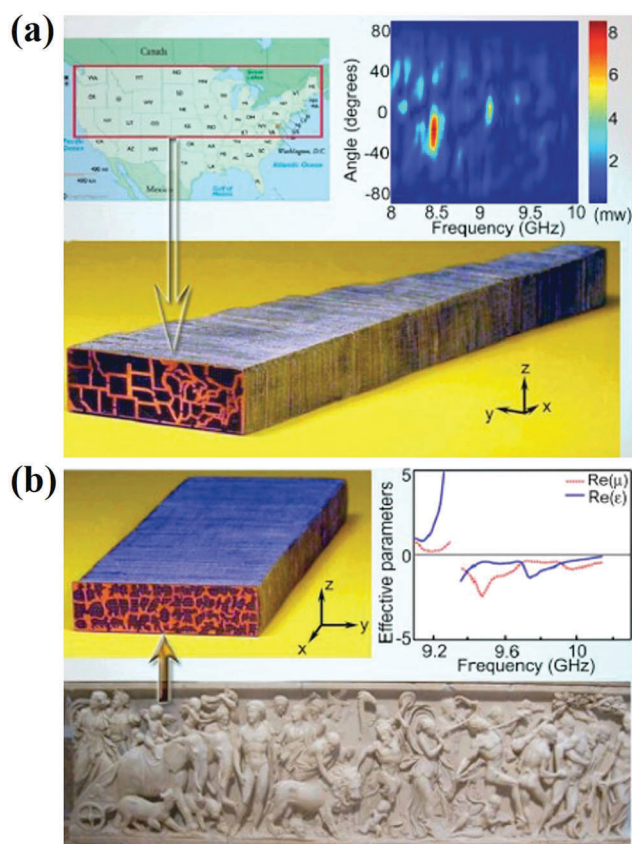

Fig. 6 The electromagnetic properties of metamaterials with randomly disorder structure.[93] (a) is the map of the northern United States of America prepared by a printed circuit board. (b) is the disorder pattern taken from the Roman sculpture sarcophagus with the triumphal procession of Dionysos. Reproduced with permission from ref. 93. Copyright (2006) AIP Publishing LLC.

Chen et al.[93] demonstrated that a negative refraction index could also be produced in metamaterials with disordered building blocks. In their experimental investigation, two different disordered metamaterials were designed and fabricated by randomizing the contour patterns deposited lithographically on circuit board materials. One of the two randomized metallic patterns was printed as the map of the northern United States of America; it was shown that the power was mainly bent to the negative angle region in the frequency range of 8.42–8.60 GHz (shown in Fig. 6a) which indicated that a negative refraction index was obtained. In order to verify the phenomenon, Chen et al. made a second pattern, which was taken from the Roman sculpture sarcophagus with the triumphal procession of Dionysos (shown in Fig. 6b). It was shown that the negative permittivity and negative permeability were simultaneously observed from 9.35–10.20 GHz, which further demonstrated that the periodicity was not a necessary condition to achieve metamaterials. It indicates that metamaterials could be realized using composite materials or disordered structure unit cells. Afterwards, Liu et al.[94] employed a nano-assembly approach to establish a sandwich-like structure metamaterial with random dendritic silver nanoparticles, which were distributed between the two dielectric media. The disordered metamaterials possessed a multi-band resonance and negative refraction index, which offered a facile and low-cost avenue to fabricate large-scale metamaterials. Moreover, Pawlak et al.[95] prepared a $TiO_2/SrTiO_3$ metamaterial with disordered SRR-like structure units via a self-organization method.

4. Metamaterials in wireless power transfer

Wireless power transfer (WPT), which transmits electric power to devices without wires or cables, has attracted extensive attention due largely to its exotic performance and promising application in the fields of electric vehicles,[36] lighting,[37] implantable medical devices[38] and mobile phone charging,[39] etc. Nevertheless, the transfer efficiency and distance are severely restricted in the WPT system with conventional materials, which has limited its development and commercial applications. Recently, it was reported that metamaterials can focus on the radio-frequency magnetic field lines of force and enhance the coupling coefficient between the resonant coils, which is beneficial to WPT transfer efficiency.[26] Hence, in this section, we focus on the advancements in WPT from the perspective of metamaterials.

4.1 Research background and basic principles of wireless power transfer

It is inevitable that undesirable energy loss is produced from conductive wires during power transmission and distribution, which leads to a decrease of power transfer efficiency.[34] As an alternative to power transmission, WPT can enhance transfer efficiency and reduce the cost without wires. In addition, compared with the traditional power transfer form,[33] WPT can improve

the safety, reliability and lifespan of the power supply system[34,35] and possesses significant applications, as mentioned above.

Actually, the feasibility of WPT was initially proposed based on Maxwell's equations in 1862,[41] which predicted that power could be transmitted from one point to another in free space by electromagnetic waves.[32] At the end of the 19th century, at the World Columbian Exposition in Chicago, Tesla demonstrated the illumination of vacuum bulbs without using wires for power transmission *via* the famous Tesla coils.[96] Afterward, he constructed the Wardenclyffe tower and attempted to broadcast approximately 300 kW of power *via* a 150 kHz radio wave from a long distance.[41,97] Unfortunately, the project was finally forced to terminate by the sponsors. In the following decades, the development of radio-waves mainly focused on wireless communication and remote sensing rather than WPT.[41] In the 1960s, Brown restarted WPT experiments and succeeded in the transmission of power by microwaves to a tethered helicopter.[98] Although the WPT technology did not obtain commercial applications due to its huge size and high cost,[41] WPT science and technology made great progress based on microwave radiation,[99–103] which was called microwave power transfer (MPT) and primarily applied for space solar power satellites.[104]

In general, the transmission methods of WPT are mainly classified into three categories according to the transfer distance and power. In the near field, a lower power can be transferred by non-radiation form without wires.[35] In the mid-range (from several centimeters to several meters) transmission, resonant coupling is used to transfer energy wirelessly.[42] For long distance (thousands of kilometers, *i.e.*, far field) and high power (megawatts to gigawatts) transmission, WPT is mainly achieved by electromagnetic wave radiation. Compared to inductive coupling, resonant coupling is more flexible in terms of tolerance to device misalignment and transfer distance.[51,105] This indicates that WPT *via* resonant coupling can be realized when the transmitter and receiver are tuned to have the same or similar resonant frequency.[106] Although the basic principle of resonant coupling has been discovered for many years, research and applications have been quite limited.[51] In fact, a WPT system with two coils was first investigated based on resonant coupling.[107] However, the transfer distance and efficiency of the two-coil system were too low to be practically applied.[108,109]

To achieve a higher transmission efficiency and longer transmission distance, three-coil[110,111] or four-coil[112–115] energy transfer systems were proposed. In 2007, Kurs *et al.*[116] established a setup (the schematic is shown in Fig. 7a) based on resonant coupling theory to realize power transfer wirelessly. In their investigation, the core part was the two self-resonant coils (*i.e.*, transmitter and receiver coils). The transmitter coil was coupled inductively to an oscillating circuit and the receiver coil was coupled inductively to a resistive load. The resonance between the two coils was attributed to the interplay between inductance and capacitance, which corresponded to the *LC* resonance.[116] Finally, a 60 watt light bulb was lit up by a resonant coupling from a distance of more than 2 m away (Fig. 7b), and the transfer efficiency was about 40%. With an increase of distance between the device coil and the bulk, the
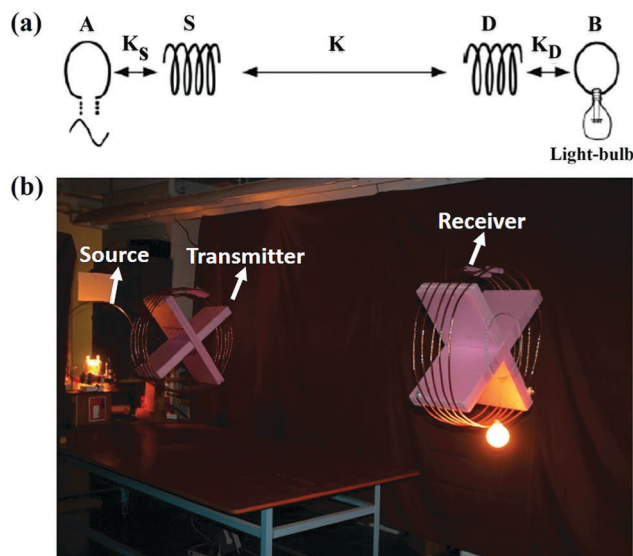

Fig. 7 Schematic of the experimental setup (a) and 60 W light–bulb being lit from 2 m away (b).[116] *A* is the driving circuit and outputs a sine wave with frequency 9.9 MHz. *S* and *D* are the source and device coils, respectively. *B* is a conductive loop attached to the load (light bulb). K_s, K_D and K are the coupling coefficients between the objects indicated by the arrows. Coils *S* and *D* are aligned coaxially. The direct couplings between *B* and *A*, and between *B* and *S*, are negligible.[116] Redrawn from ref. 116.

efficiency gradually reduced. This study played a significant role in the development of WPT, especially in non-radiation mid-range transmission.

However, the main disadvantage of the wireless energy transmission structure is that the efficiency decays rapidly with an increase of transmission distance. Hence, there is an urgent requirement to improve the transmission efficiency. In recent years, extensive attention has been paid to enhance the efficiency in the resonant coupling WPT system.[34] There are several methods to effectively improve the transmission efficiency, such as optimum frequency adjustment,[35,117] controlling resonant parameters,[34] coupling manipulation,[118,119] introducing relay coils,[120,121] using antiparallel resonant loops[122,123] and adaptively matching with multi-loop coils,[124,125] *etc.* Even though these approaches could improve the transfer efficiency and distance more or less, achieving a higher efficiency and practical applications, it was limited for a large coupling distance. It is worth noting that Wang *et al.*[51,126] designed a metamaterial to successfully increase the transfer efficiency, which opened a novel approach to promote the development of WPT.

4.2 Theoretical research of metamaterials in wireless power transfer

The transfer efficiency of a resonant coupling WPT system mainly depends on two significant factors, *i.e.*, the quality factor *Q* of the resonant coils and the coupling coefficient *k* between coils. Generally, a higher *Q* means a lower loss during the energy transmission and a larger *k* represents a higher coupling rate, which contributes to improve the efficiency.[40] Hence, based on the above considerations, Wang *et al.*[126] theoretically proposed
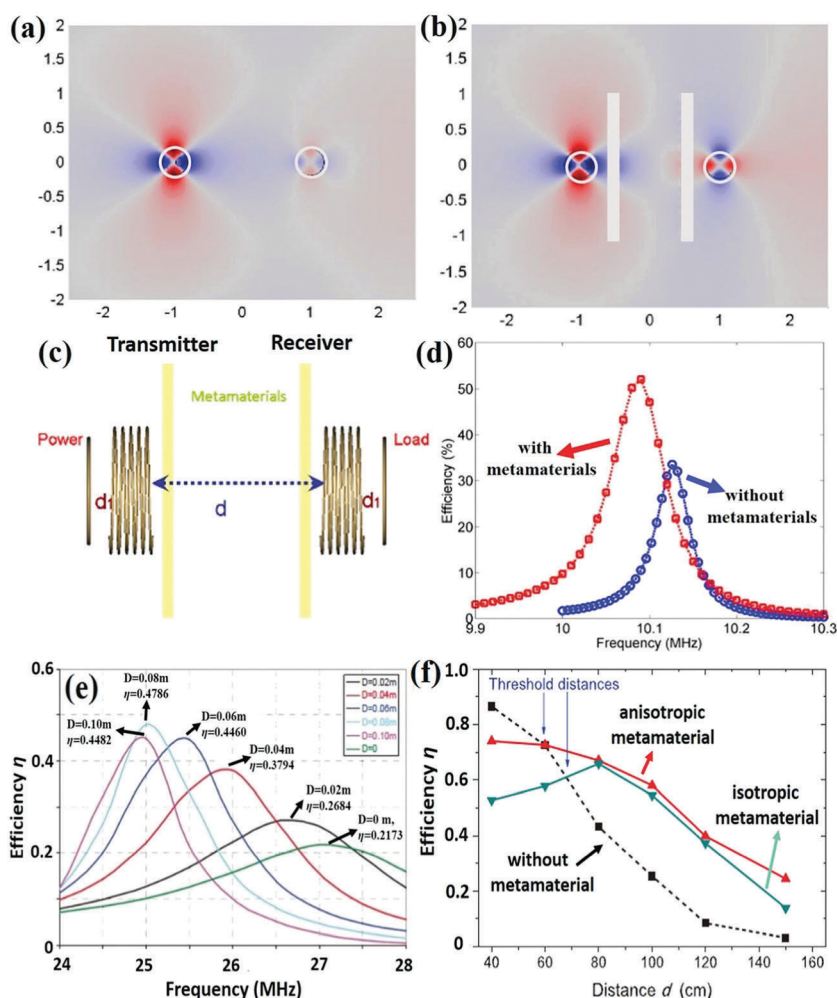
Fig. 8 The simulated electric field distribution of coupled dielectric resonators (a) without and (b) with metamaterial slabs. An illustration of the wireless power transfer system with metamaterials (c). The calculated efficiency of the system with and without the metamaterial slabs as a function of frequency (d).[40] (e and f) Show the relationship between transfer efficiency and transfer distance.[127,128] Redrawn from ref. 40, 127 and 128.

to enhance the coupling coefficient between transmitter and receiver, and improve the transfer efficiency taking advantage of negative-index metamaterials. It can be seen that a strong electric field is localized at the resonant coils and the field strength outside the resonant coils decays exponentially (Fig. 8a), indicating that the near field is decaying away from the resonators.[40] Similarly, the resonant mode is excited in the second resonator with a smaller amplitude. When the metamaterial slabs are introduced (Fig. 8b), a similar resonant mode is also observed. However, under the action of the metamaterial slabs, the field is amplified and the evanescent field is extended further toward the second resonator compared with that in Fig. 8a. A schematic of the WPT system with metamaterials is shown in Fig. 8c. The source coil is coupled resonantly to the sink coil, and the two slabs with both ε and μ equal to -1 are fixed between the two resonant coils. For a given constant distance d between the two coils, the distance d_1 between the power (load) loop and the source (sink) coil was adjusted to optimize the coupling coefficient in order to achieve the highest efficiency. When other parameters are the same as in a WPT

system without metamaterials, it was shown that the calculated peak efficiency is more than 50% by introducing the two metamaterial slabs into the coils, which is a significant increase compared with that of the original system (Fig. 8d). Additionally, the efficiency peak is shifted a little due to the coupling of the slabs with the resonators.[126] Therefore, this indicates that the metamaterials can enhance the transfer efficiency, and more attention needs to be paid to WPT based on metamaterials. As shown in Fig. 8e, it was demonstrated that the transfer efficiency initially increased and then decreased with the increase of transfer distance.[127] When the transfer distance was too close, the coupling coefficient between the receiver and transmitter coils was not high enough, which resulted in a relatively low transfer efficiency. With an increase of transfer distance, the coupling coefficient gradually enhanced and reached a maximum, and the highest transfer efficiency was obtained. Further increasing the distance, the energy decayed fast and the coupling coefficient was reduced as well, so the transfer efficiency decreased. As shown in Fig. 8f, without metamaterials for WPT,[128] the efficiency gradually decreased with an increase of distance.

When injecting metamaterials into the two coils, the transfer efficiency showed a similar variation trend, compared with that in Fig. 8e. Moreover, this indicates that anisotropic metamaterials possess a higher efficiency than anisotropic metamaterials.

It has been shown that negative-index metamaterials can be used to refocus the flux at the receiver and to enhance the coupling coefficient, both of which contribute to the transfer efficiency. However, on the other side, metamaterials are usually composed of some conducting circuits and produce losses, which is detrimental to the development and applications of energy transmission.[40,129] Hence, in order to find out the combined effects of metamaterials on energy transfer performance, Urzhumov et al.[130] made detailed investigations and reliable calculations. They proposed a circuit model of the inductive coupling between two coils and one metamaterial slab. The coils were simplified as point magnetic dipoles, and the metamaterial slab was assumed to be infinitely large.[40] Urzhumov et al.[130] revealed that, even with a realistic magnetic loss tangent of 0.1 of the metamaterial slab, the power transfer efficiency with the slab can be an order of magnitude greater than the efficiency without the slab. It was verified that, with a metamaterial slab as a perfect lens, the mutual inductance can be increased significantly and enhance the transfer efficiency.[40] Moreover, it was demonstrated that the efficiency can be further enhanced by employing metamaterials with a large anisotropy ratio.

As mentioned above, negative refraction behavior in a metamaterial lens can refocus the flux and increase the mutual inductive coupling between the coils,[26] thereby improving the transfer efficiency. Further, Huang et al.[129] investigated the impact of the finite size of the coils and the metamaterial lens

(superlens) on WPT efficiency. The enhancement factor ρ was defined as the ratio of the calculated mutual inductance and theoretical mutual inductance in a vacuum, evaluating the enhancement of mutual coupling with the superlens. A two-coil coupling WPT system with a superlens is shown in Fig. 9a; W is the diameter and L is the thickness of the superlens, and the distance between source and receiver coils is D. The superlens produces surface waves around its surface. The effect of the finite coil size on the mutual inductance without the slab is investigated in Fig. 9b; with increasing the radius of coils, the enhancement factor gradually decreased and reduced sharply when the coil size reached about $0.001\lambda_0$ (the wavelength in free space). This indicates that the magnetic flux is difficult to focus when the applied coils have a larger size, which results in a decrease of transfer efficiency. In addition, the effect of the superlens size was further clarified. Fig. 9c presents that the magnetic field intensity in the receiver coil, indeed, increases as the thickness of the superlens increases with the overall distance between the source and receiver coils fixed at $D = 0.5$ m.[129] The surface wave (i.e., evanescent wave) decays exponentially away from the superlens, which leads to a lower transfer efficiency. When a thicker superlens is placed in the coils, the evanescent wave can be enhanced and the coupling coefficient can be improved. The dependence of the enhancement factor on the diameter of the superlens is shown in Fig. 9d. The enhancement factor increases rapidly and saturates when the superlens diameter W reaches D (the distance between the two resonant coils). When the superlens diameter is below a certain size, the superlens cannot produce a two-dimensional focus and the electromagnetic field excited on the edge of the lens will
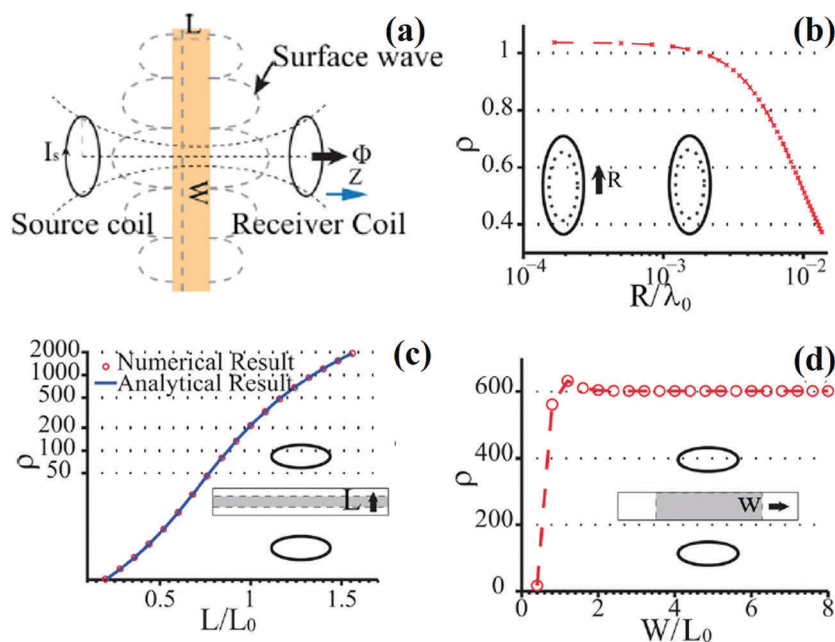

Fig. 9 Schematic of a WPT system with a superlens (a). W is the diameter and L is the thickness of the superlens; I_s is the current in the source coil and Φ is the magnetic flux density. The effect of finite coil size on the mutual inductance without the superlens (b). The dependences of enhancement factor on the superlens thickness L for a fixed intercoil distance (c), where $L_0 = D/2$ is the optimum superlens thickness. Mutual inductance enhancement as a function of the superlens diameter W (d).[129] Reproduced with permission from ref. 129. Copyright (2012) AIP Publishing LLC.

produce uncontrolled focusing or defocusing. As shown in Fig. 9d, the enhancement factor becomes larger than its asymptotic value for certain superlens widths. Subsequently, the enhancement factor saturates for larger widths, where any influence of the superlens termination on the surface resonance modes becomes negligible.[129] This suggests that the superlens dimensions play a significant role in focusing the flux and enhancing the energy transfer efficiency. According to the theoretical calculation and analysis, it is feasible to achieve the maximum efficiency enhancement for WPT by carefully choosing the dimensions and permeability magnitude.

4.3 Enhancement of wireless power transfer efficiency with metamaterials

Although much attentions was paid on improving the efficiency of WPT systems with metamaterials in theory, the experiment realization of WPT with metamaterials was first achieved by Wang et al.[51] in 2011. This indicated that the magnetic field and electric field can be decoupled in a deep subwavelength limit, so either permittivity or permeability is required to be negative to achieve evanescent wave amplification.[6,26] Generally, the wavelength in the near field is larger than the size of the WPT system, which requires a deep subwavelength limit. Consequently, Wang et al.[51] used a metamaterial slab, which had a negative permeability but a positive permittivity, for evanescent wave amplification and efficiency enhancement. Fig. 10a shows the structure of metamaterials slab and the inset shows the structure of the unit cell. The cell was fabricated by a printed circuit board method. After the metamaterial slab was put into the WPT system, the distances between the loop antennas and the associated coil resonators were readjusted in order to achieve an optimal matching for the power transfer. The strong response resulted from the resonance of the structure, which could be effectively considered as an LC resonator.[131] The multi-turn metal wires are responsible for the inductance L, and the capacitance C comes mainly from the "plate capacitor" formed by the two sides of the metal structure.[40] Taking the magnetic field direction into consideration, it is sufficient to use an anisotropic metamaterial with a negative magnetic response just along the magnetic field direction. The anisotropic metamaterial is constructed by removing the inter-locked structures of the metamaterial slab and leaving only two surfaces (in the inset of Fig. 10b), which are separated by a distance $t = 2$ cm to achieve the optimal coupling resonant.[51] The power transfer efficiency of different system configurations is shown in Fig. 10b. The power transfer efficiency of the WPT system with a three dimensional (3D) metamaterial is nearly twice that of the original system without a metamaterial. Meanwhile, the efficiency peak is shifted to a higher frequency region owing to the mutual coupling between the metamaterial and the spirals and antennas. When the anisotropic metamaterial was placed into the WPT system, the maximum efficiency reached up to almost 50%, much higher than that of the other two systems. Compared with the 3D metamaterial, the anisotropic metamaterial possesses a lower loss due largely to the removal of unnecessary structures, which bring about loss. Fig. 10c and d present the practical
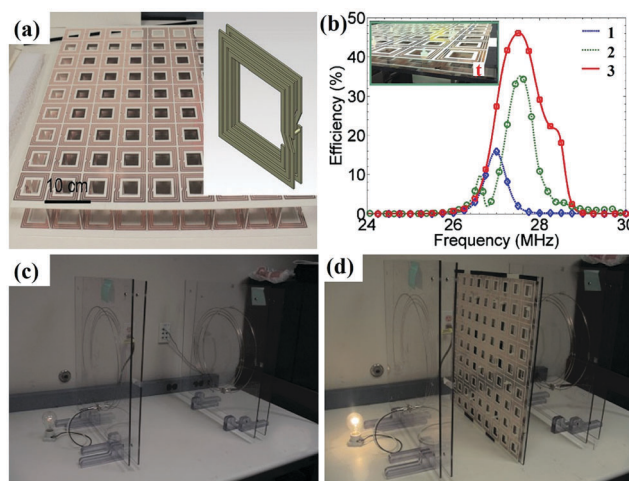

Fig. 10 The three dimensional structure of the metamaterial (a); the inset shows the structure of the unit cell. (b) Shows the power transfer efficiency of different system configurations: 1 original system without the metamaterial, 2 with the 3D metamaterial, and 3 with the anisotropic metamaterial. The inset in (b) is the anisotropic metamaterial with a space of thickness $t = 2$ cm. WPT experiments to light a 40 W light bulb with or without anisotropic metamaterial are shown in (c) and (d), respectively.[51] Reproduced with permission from ref. 51. Copyright (2011) AIP Publishing LLC.

WPT setups with (Fig. 10d) and without (Fig. 10c) the anisotropic metamaterial. When there is no metamaterial, the 40 watt light bulb barely glows. After the anisotropic metamaterial is applied, the light bulb is much brighter, which demonstrates that the efficiency is, indeed, improved significantly by using the metamaterial in a WPT system. Moreover, Fan et al.[132] constructed a WPT system integrated with metamaterials to improve the efficiency. This demonstrated that the WPT system with metamaterials can significantly improve the transfer efficiency and transfer distance. When three or four metamaterial slabs were placed between the source and receiver coils, the transfer efficiency was enhanced obviously. By adjusting the distance between the metamaterial slab and coil, the optimal transfer efficiency could be achieved.

Since Wang et al.[51] successfully enhanced the power transfer efficiency by taking advantage of a metamaterial, the development of metamaterials has been promoted towards commercial applications in the WPT field based on metamaterials.[133-135] Recently, Kang et al.[136] proposed a novel three-coil WPT system with a metamaterial array to improve the transfer efficiency for a laptop computer. Due to the removal of the receiver coil, the three-coil WPT system (Fig. 11a) has a planar receiver and can be applied in mobile electronic devices, such as mobile phones and laptops, etc. When the metamaterial array was introduced, the transfer efficiency was increased by 27% at a transfer distance of 50 cm (Fig. 11b).

Generally, the electrical devices have a complicated environment for transferring power wirelessly due to one or several ground planes.[136] In order to illustrate a practical situation, a ground plane was introduced behind the load coil with a gap (Fig. 11c). To further reveal the impact of the ground plane (i.e., the ground impact) on the WPT system with a metamaterial

2936 | J. Mater. Chem. C, 2018, 6, 2925–2943

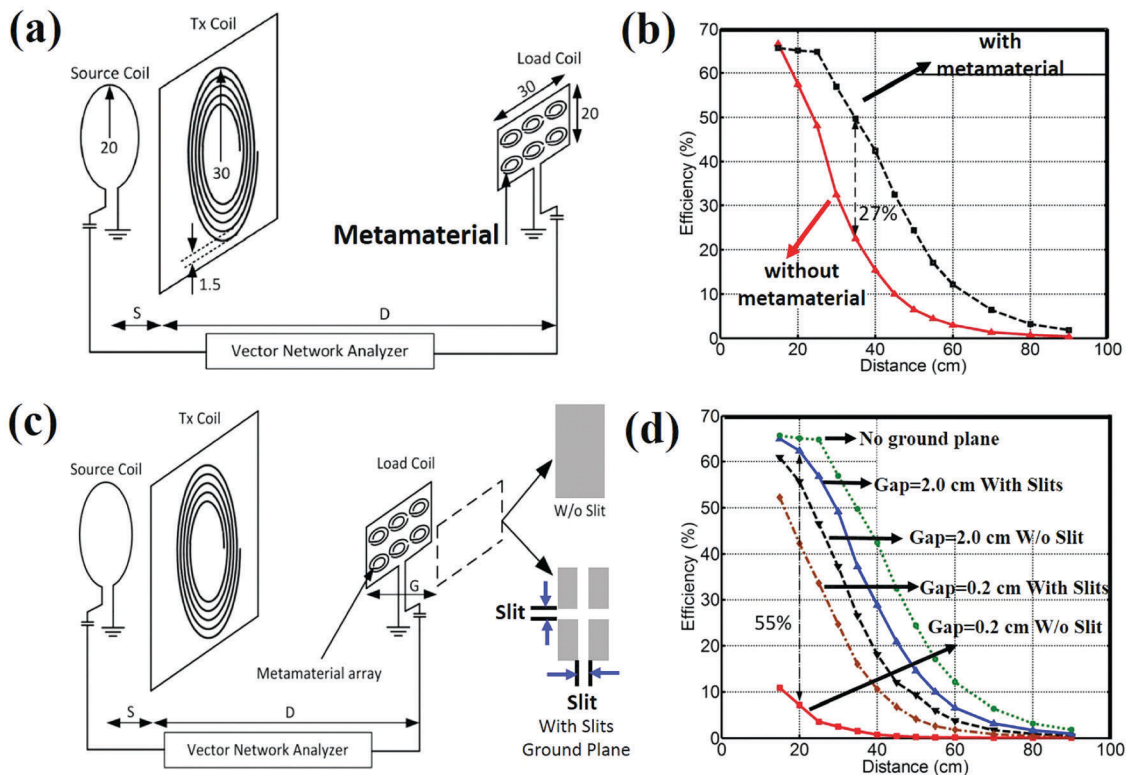This journal is © The Royal Society of Chemistry 2018

Fig. 11 Schematic of three-coil WPT system (a). S and D are the distances between the source and Tx coil (the transmitted coil), and between the Tx and the load coil, respectively. The measured transfer efficiency with and without (W/o) metamaterial array (b). The investigation of the ground impact on transfer efficiency (c). G is the gap distance between the load coil and ground plane. The measured efficiency of the three-coil WPT system with the metamaterial array for different cases (d).[136] Redrawn from ref. 136.

array, several cases were examined as follows: (1) ground plane with and without slits; (2) with a 0.2 cm or 2 cm gap.[136] This exhibited that, when the gap is small (0.2 cm) and the ground plane is without slits, the transfer efficiency is much lower, which is attributed to the reflection of the magnetic field due to the ground plane. When the gap was increased or slits were made on the ground plane, the transfer efficiency became obviously enhanced throughout the transfer distance. This can be explained as that the magnetic field can easily pass through the load coil, leading to a higher efficiency. By adjusting the gap and slit size, the maximal improvement of transfer efficiency was about 55% at the transfer distance D = 20 cm (Fig. 11d). The ground impact made an adverse effect on the transfer efficiency, compared with that without a ground plane (the dotted green lines in Fig. 11d). It is feasible to reduce the undesirable ground impact by making slits on the ground plane or increasing the gap.

In order to simulate practical WPT applications, Kang et al.[136] fabricated a laptop model with a screen and a keyboard (Fig. 12), which are both inserted with a ground plane. Additionally, the dimensions of the modeled laptop are consistent with those of a real laptop. The transfer efficiency was systematically investigated when the metamaterial array, load coil and ground plane were located in the screen and keyboard parts, respectively. The load coil, metamaterial array and ground plane were put in the screen side and the angles of the screen were tuned at 45°, 90° and 135° compared to the keyboard (Fig. 12a). The transfer efficiencies in

the different cases are displayed in Fig. 12b. It was shown that the efficiency enhances significantly when metamaterial array was employed and slits were made on the ground. Furthermore, the angles of the screen played a great role in the power transfer efficiency. The optimal efficiency is observed when the angle is at 90°, which is ascribed to the fact that the magnetic field is mostly coupled to the load coil at this angle. When the metamaterial array, load coil and ground plane were inserted in the keyboard part, and the laptop was placed on the Tx coil with a given gap (Fig. 12c), the transfer efficiencies for different cases were measured. Subsequently, the dependence of efficiency on the position of the laptop, which was removed from the center of the Tx coil to the outer radius, was studied in detail (Fig. 12d). The angle between the keyboard and the screen of the laptop model was kept at 135°. Similarly, the metamaterial array and slits on the ground plane contributed to the improvement of efficiency. When the efficiency reached its highest value, the optimized position was 15 cm from the center of the Tx coil, and the transfer efficiency dramatically decreased when the laptop model was moved to the outer region of the spiral.[136] This research offers an efficient WPT system and has promising commercial prospects in mobile electronic devices.

4.4 Improvement of wireless power transfer distance with metamaterials

Although the WPT technique has made great progress in enhancing the efficiency,[137–140] there are still obstacles to be
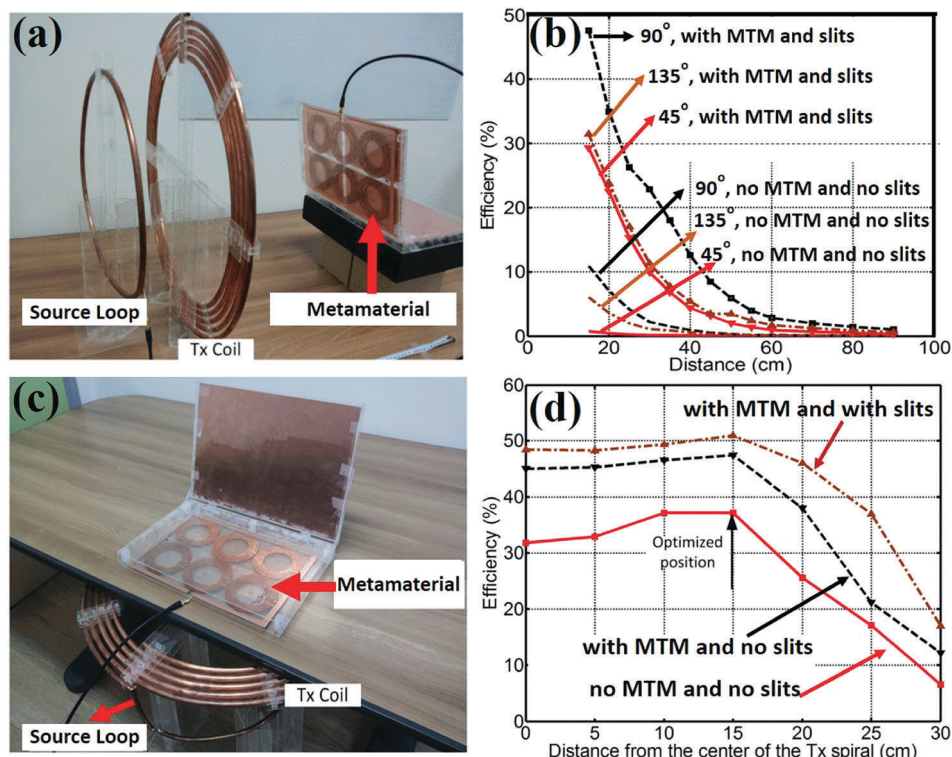
Fig. 12 Experimental WPT setup with the metamaterial array located in the screen part (a). The effect of the load coil angle on the WPT efficiency for different cases (b). The experimental WPT setup with the metamaterial array placed in the keyboard (c). The effect of the load coil position on the WPT efficiency for different cases (d). MTM is the abbreviation of metamaterial.[136] Redrawn from ref. 136.

overcome for practical applications, especially the limitation of transfer distance.[141] It is necessary for the improvement of WPT efficiency to attain a strong coupling between the transmitter and receiver coils. However, the coupling coefficient usually decreases sharply with an increase of transfer distance.[141] The efficiency η of a WPT system without a metamaterial slab decreases with increasing distance d quickly, namely, $\eta \sim d^{-6}$, which means that the energy loss quickly approaches 100% and limits the practical application of the WPT technique.[130,142] The negative permeability slab served to focus on the flux generated in the source coil to the receiver coil, leading to an increase in the mutual inductive coupling between the coils. The superlens, whose permittivity and permeability both took on the value of -1,[143] could refocus the propagating far-field waves and non-propagating near-field waves, which was different from the conventional lens.[144] Hence, a superlens based on metamaterials could be used to enhance the power transfer distance by controlling and manipulating the near-fields wave that would decay rapidly away from a source.[142] Lipworth et al.[142] proposed to increase the transfer distance with a magnetic metamaterial superlens based on previous theoretical investigations.[129,130] These indicated that a metamaterial with a finite and realistic loss could help deliver magnetic flux and boost the transfer distance (Fig. 13a). When there was no metamaterial between the two coils, the transfer efficiency rapidly decreased with an increase of transfer distance due to the exponential decay of inductive coupling between two coils.

When the metamaterial superlenses were put into the coils, the transfer efficiency could retain a relatively high value when the transfer distance exceeded a certain threshold. In addition, the transfer efficiency was gradually reduced when the loss from the metamaterial was enhanced. In order to further increase the transfer distance based on a WPT system, Zhu et al.[141] employed superscatterers (ss), i.e., metamaterial, to realize a distant and wide range wireless power transfer. As shown in Fig. 13b, the efficiency reached up to 97.2% at a 2.8 m distance when the receiver was close to the amplified image of the emitter. It is worth noting that the transfer efficiency presented a relatively high value (50%) in a wide transfer range. Compared with the transfer efficiency in an ordinary WPT system without a metamaterial, the metamaterial contributed to improve the transfer distance, which could promote commercial applications. This indicates that metamaterials can focus the magnetic flux under the action of an external electromagnetic field. During the power transfer, metamaterials could be regarded as an energy repeater, which results in a relatively high coupling coefficient and enhances the transfer efficiency, compared with that of an ordinary WPT without metamaterials. When the transfer distance was about 3 m, the resonant frequency for metamaterials was reached. A strong response was produced from the periodic structure of the metamaterials, which could be effectively considered as an LC resonator, where the inductance came from the multi-turn metal wires, and the capacitance came mainly from
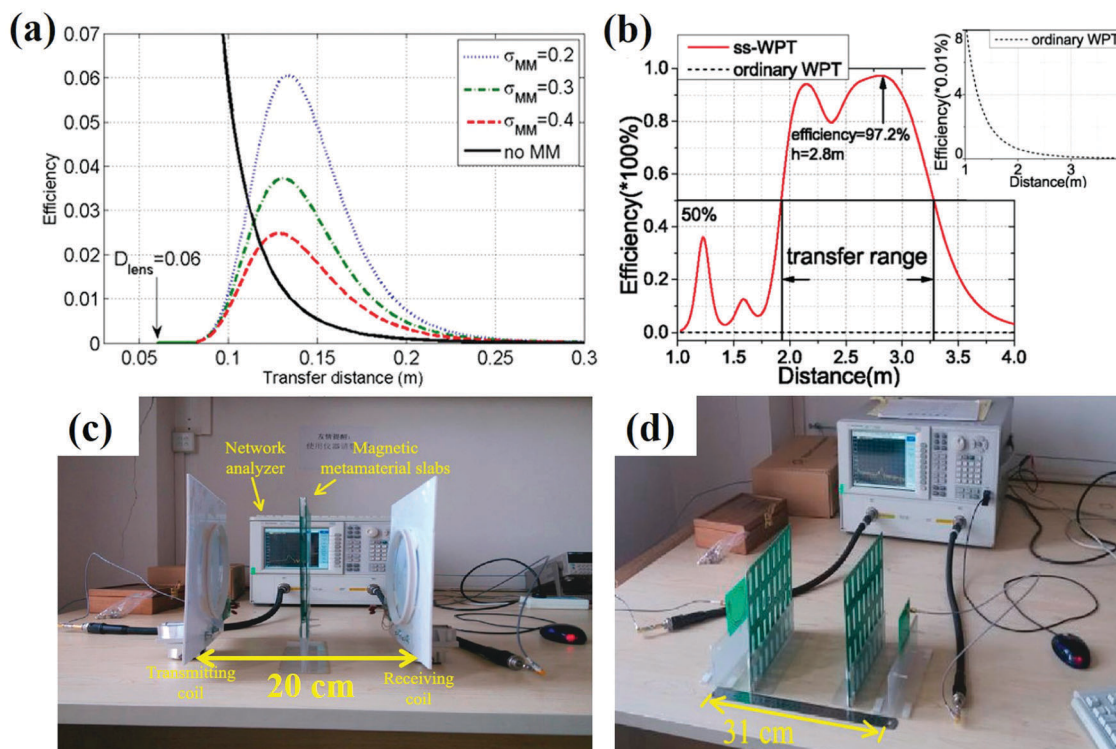
2938 | J. Mater. Chem. C, 2018, 6, 2925–2943

This journal is © The Royal Society of Chemistry 2018

Fig. 13 Calculated transfer efficiency in the WPT system with/without a 6 cm metamaterial superlens (a).[142] σ_{MM} is the loss in metamaterial. The transfer efficiency with/without a superscatterer (ss) metamaterial at different transfer distances (b).[141] Comparison of transmission distances in WPT systems with a single (c) and two metamaterial slabs (d).[146] Reproduced with permission from ref. 141 and 142 (Open Access) and 146 (Open Access). Copyright (2016) AIP Publishing LLC, (2014) Springer Nature, (2015) AIP Publishing LLC.

the "plate capacitor". Therefore, a very high transfer efficiency was observed at the resonant location.[145] Interestingly, Zhang et al.[146] proposed a novel WPT structure with two metamaterial slabs to enhance the transfer distance. The two coils placed 20 cm apart were connected to a network analyzer to determine the resonant frequency of the metamaterial slab, which was placed in the center of the two coils (Fig. 13c).[146] When two metamaterial slabs were inserted into the two coils, the transfer distance could be extended from the original 20 cm to 31 cm (Fig. 13d), which proved that the metamaterial could effectively enhance the transfer distance.

5. Conclusions and perspective

Compared with a traditional WPT system, although it produces some inevitable energy loss in the novel WPT system with metamaterials, the transfer efficiency can be obviously enhanced, which is attributed to the fact that metamaterials with a negative permeability behavior can refocus the flux and increase the mutual inductive coupling between the source and receiver coils. In addition, when the metamaterial is placed between these two coils, the transfer distance can be significantly enlarged by controlling and manipulating the near-fields wave, which usually decays rapidly away from a source. This indicates that the transfer efficiency and distance can be further enhanced when the number of metamaterial slabs is increased.

Indeed, metamaterials can enhance the transfer efficiency and transfer distance due to their unique properties. However, it is worth noting that the investigations on metamaterials for WPT applications are still in the basic research stage. Hence, most research about the application of metamaterials in WPT is reported in the field of lighting and laptops, rather than electric vehicles, implantable biomedical devices and high-power portable mobile devices, etc. According to the basic principle, it is demonstrated that WPT via resonant coupling can be realized when the transmitter and receiver are tuned to have the same or similar resonant frequency. Hence, WPT based on metamaterials has great potential applications in the field of electric vehicles, implantable biomedical devices and high-power portable mobile devices, which provides a novel approach to more promising applications of WPT based on metamaterials.

Although extensive investigations have been made into an enhanced WPT efficiency and enlarged distance based on metamaterials,[147–151] there are still some challenges to overcome.[152] In general, metamaterials are usually prepared with a metallic component and produce a large energy loss, which limits their development and applications. Therefore, there is an urgent requirement to achieve metamaterials with a lower loss to improve the WPT performance. In the future, the focus should be on the structural configurations and fabrication process of metamaterials to make a breakthrough.[28] Moreover, the WPT technique mainly focuses on low power applications; it is significant to enlarge the transfer power (up to few kW) at a

This journal is © The Royal Society of Chemistry 2018

J. Mater. Chem. C, 2018, 6, 2925–2943 | 2939

low frequency region (from 10 kHz up to 20 MHz), to promote commercial applications in the fields of electric vehicles and energy storage. Hence, in future studies, more attention should be paid to obtain high power metamaterials at a low frequency region. On the other hand, dynamically tunable metamaterials is an interesting field to be explored.[152]

As discussed above, metamaterials with negative permeability can refocus the flux and result in a significant enhancement of transfer efficiency in a WPT system.[26] Recently, a negative permeability behavior was reported to be achieved in natural magnetic materials due to magnetic resonance.[153,154] The negative permeability properties were observed in random composites with ferrite[44,61,155] or ferromagnetic metal particles, such as nickel,[50] iron[156] and cobalt,[48] *etc.* random composites, which are also called metacomposites due to their unique electromagnetic property,[157] and possess a simple preparation approach, low manufacture cost and broadband application,[158–163] compared with metamaterials consisting of periodic structure units. It is feasible to realize a tunable negative permeability and controllable WPT property by designing the composition and tailoring the microstructure. Therefore, as an alternative for metamaterials, random composites with a negative permeability behavior could be promising candidates for WPT development and commercial applications.

Conflicts of interest

There are no conflicts to declare.

Acknowledgements

References

1 D. R. Smith, J. B. Pendry and M. C. Wiltshire, *Science*, 2004, **305**, 788–792.

2 S. H. Lee, C. M. Park, Y. M. Seo and C. K. Kim, *Phys. Rev. B: Condens. Matter Mater. Phys.*, 2010, **81**, 241102.

3 A. A. Zharov, I. V. Shadrivov and Y. S. Kivshar, *Phys. Rev. Lett.*, 2003, **91**, 037401.

4 K. Sun, R. Fan, Z. Zhang, K. Yan, X. Zhang, P. Xie, M. Yu and S. Pan, *Appl. Phys. Lett.*, 2015, **106**, 172902.

5 V. G. Veselago, *Phys.-Usp.*, 1968, **10**, 509.

6 J. B. Pendry, *Phys. Rev. Lett.*, 2000, **85**, 3966.

7 R. A. Shelby, D. R. Smith and S. Schultz, *Science*, 2001, **292**, 77–79.

8 D. Schurig, J. Mock, B. Justice, S. A. Cummer, J. B. Pendry, A. Starr and D. Smith, *Science*, 2006, **314**, 977–980.

9 B. Edwards, A. Alù, M. G. Silveirinha and N. Engheta, *Phys. Rev. Lett.*, 2009, **103**, 153901.

10 F. Ding, Y. Cui, X. Ge, Y. Jin and S. He, *Appl. Phys. Lett.*, 2012, **100**, 103506.

11 S. Zhang, W. Fan, N. Panoiu, K. Malloy, R. Osgood and S. Brueck, *Phys. Rev. Lett.*, 2005, **95**, 137404.

12 X. Liu, T. Starr, A. F. Starr and W. J. Padilla, *Phys. Rev. Lett.*, 2010, **104**, 207403.

13 Y. Avitzour, Y. A. Urzhumov and G. Shvets, *Phys. Rev. B: Condens. Matter Mater. Phys.*, 2009, **79**, 045131.

14 J. Yao, Z. Liu, Y. Liu, Y. Wang, C. Sun, G. Bartal, A. M. Stacy and X. Zhang, *Science*, 2008, **321**, 930.

15 I. I. Smolyaninov, Y. J. Hung and C. C. Davis, *Science*, 2007, **315**, 1699–1701.

16 V. M. Shalaev, *Nat. Photonics*, 2007, **1**, 41–48.

17 N. Liu, H. Guo, L. Fu, S. Kaiser, H. Schweizer and H. Giessen, *Nat. Mater.*, 2008, **7**, 31–37.

18 G. Dolling, M. Wegener, C. M. Soukoulis and S. Linden, *Opt. Lett.*, 2007, **32**, 53–55.

19 Y.-S. Lin and C. Lee, *Appl. Phys. Lett.*, 2014, **104**, 251914.

20 S. Lee, S. Kim, T. T. Kim, Y. Kim, M. Choi, S. H. Lee, J. Y. Kim and B. Min, *Adv. Mater.*, 2012, **24**, 3491–3497.

21 A. M. Hawkes, A. R. Katko and S. A. Cummer, *Appl. Phys. Lett.*, 2013, **103**, 163901.

22 O. M. Ramahi, T. S. Almoneef, M. AlShareef and M. S. Boybay, *Appl. Phys. Lett.*, 2012, **101**, 173903.

23 J. Valentine, J. Li, T. Zentgraf, G. Bartal and X. Zhang, *Nat. Mater.*, 2009, **8**, 568–571.

24 X. Ni, Z. J. Wong, M. Mrejen, Y. Wang and X. Zhang, *Science*, 2015, **349**, 1310–1314.

25 X. Zhang and Z. Liu, *Nat. Mater.*, 2008, **7**, 435–441.

26 M. J. Freire, R. Marques and L. Jelinek, *Appl. Phys. Lett.*, 2008, **93**, 231108.

27 M. A. Lopez, M. J. Freire, J. M. Algarin, V. C. Behr, P. M. Jakob and R. Marqués, *Appl. Phys. Lett.*, 2011, **98**, 133508.

28 Z. Chen, B. Guo, Y. Yang and C. Cheng, *Phys. Rev. B: Condens. Matter Mater. Phys.*, 2014, **438**, 1–8.

29 C. M. Soukoulis and M. Wegener, *Nat. Photonics*, 2011, **5**, 523–530.

30 S. Walia, C. M. Shah, P. Gutruf, H. Nili, D. R. Chowdhury, W. Withayachumnankul, M. Bhaskaran and S. Sriram, *Appl. Phys. Rev.*, 2015, **2**, 011303.

31 S. Jahani and Z. Jacob, *Nat. Nanotechnol.*, 2016, **11**, 23–36.

32 W. C. Brown, *Sol. Energy*, 1996, **56**, 3–21.

33 Y. Huang, H. J. Tang, E. C. Chen and C. Yao, *AIP Adv.*, 2013, **3**, 072134.

34 S. D. Barman, A. W. Reza, N. Kumar, M. E. Karim and A. B. Munir, *Renewable Sustainable Energy Rev.*, 2015, **51**, 1525–1552.

35 A. P. Sample, D. T. Meyer and J. R. Smith, *IEEE Trans. Ind. Electron.*, 2011, **58**, 544–554.

36 B. M. Faruk, U. S. Jawarkar, T. G. Pal and A. S. Gugliya, *IARJSET*, 2017, **4**, 111–119.

37 W. Zhong, C. K. Lee and S. R. Hui, *IEEE Trans. Ind. Electron.*, 2013, **60**, 261–270.

38 A. Kim, M. Ochoa, R. Rahimi and B. Ziaie, *IEEE Access*, 2015, **3**, 89–98.

39 Q. Li and Y. C. Liang, *IEEE Trans. Power Electron.*, 2015, **30**, 6203–6212.

2940 | *J. Mater. Chem. C*, 2018, **6**, 2925–2943

This journal is © The Royal Society of Chemistry 2018

40 B. Wang, W. Yerazunis and K. H. Teo, *Proc. IEEE*, 2013, **101**, 1359–1368.

41 A. Tomar and S. Gupta, *Int. J. Eng.*, 2012, **1**, 1–8.

42 B. Zhu, J. Li, W. Hu and X. Gao, *Int. J. U and E Ser. Sci. Technol.*, 2015, **8**, 257–272.

43 X. Wei, Z. Wang and H. Dai, *Energies*, 2014, **7**, 4316–4341.

44 K. Sun, Z. Zhang, R. Fan, M. Chen, C. Cheng, Q. Hou, X. Zhang and Y. Liu, *RSC Adv.*, 2015, **5**, 61155–61160.

45 S. Chui and L. Hu, *Phys. Rev. B: Condens. Matter Mater. Phys.*, 2002, **65**, 144407.

46 K. Sun, Z. Zhang, L. Qian, F. Dang, X. Zhang and R. Fan, *Appl. Phys. Lett.*, 2016, **108**, 061903.

47 A. Boltasseva and H. A. Atwater, *Science*, 2011, **331**, 290–291.

48 X. Wang, Z. Shi, M. Chen, R. Fan, K. Yan, K. Sun, S. Pan and M. Yu, *J. Am. Ceram. Soc.*, 2014, **97**, 3223–3229.

49 N. Engheta and R. W. Ziolkowski, *Metamaterials: physics and engineering explorations*, John Wiley & Sons, 2006.

50 Z. Shi, R. Fan, Z. Zhang, L. Qian, M. Gao, M. Zhang, L. Zheng, X. Zhang and L. Yin, *Adv. Mater.*, 2012, **24**, 2349–2352.

51 B. Wang, K. H. Teo, T. Nishino, W. Yerazunis, J. Barnwell and J. Zhang, *Appl. Phys. Lett.*, 2011, **98**, 254101.

52 R. Shelby, D. Smith, S. Nemat-Nasser and S. Schultz, *Appl. Phys. Lett.*, 2001, **78**, 489–491.

53 J. Pendry, A. Holden, W. Stewart and I. Youngs, *Phys. Rev. Lett.*, 1996, **76**, 4773.

54 M. Gao, Z. c. Shi, R. h. Fan, L. Qian, Z. d. Zhang and J. y. Guo, *J. Am. Ceram. Soc.*, 2012, **95**, 67–70.

55 E. Arslan, Y. Şafak, Ş. Altındal, Ö. Kelekçi and E. Özbay, *J. Non-Cryst. Solids*, 2010, **356**, 1006–1011.

56 A. Islam Khan, D. Bhowmik, P. Yu, S. Joo Kim, X. Pan, R. Ramesh and S. Salahuddin, *Appl. Phys. Lett.*, 2011, **99**, 113501.

57 S. Linden, C. Enkrich, M. Wegener, J. Zhou, T. Koschny and C. M. Soukoulis, *Science*, 2004, **306**, 1351–1353.

58 Q. Zhao, L. Kang, B. Du, H. Zhao, Q. Xie, X. Huang, B. Li, J. Zhou and L. Li, *Phys. Rev. Lett.*, 2008, **101**, 027402.

59 Q. Zhao, J. Zhou, F. Zhang and D. Lippens, *Mater. Today*, 2009, **12**, 60–69.

60 T. Kasagi, T. Tsutaoka and K. Hatakeyama, *Appl. Phys. Lett.*, 2006, **88**, 172502.

61 T. Tsutaoka, K. Fukuyama, H. Kinoshita, T. Kasagi, S. Yamamoto and K. Hatakeyama, *Appl. Phys. Lett.*, 2013, **103**, 261906.

62 W. Cai, U. K. Chettiar, A. V. Kildishev and V. M. Shalaev, *Nat. Photonics*, 2007, **1**, 224–227.

63 H. Chen, L. Ran, J. Huangfu, X. Zhang, K. Chen, T. M. Grzegorczyk and J. A. Kong, *Appl. Phys. Lett.*, 2005, **86**, 151909.

64 J. Huangfu, L. Ran, H. Chen, X.-M. Zhang, K. Chen, T. M. Grzegorczyk and J. A. Kong, *Appl. Phys. Lett.*, 2004, **84**, 1537–1539.

65 C. García-Meca, R. Ortuno, F. Rodríguez-Fortuño, J. Martí and A. Martínez, *Opt. Lett.*, 2009, **34**, 1603–1605.

66 S. P. Burgos, R. De Waele, A. Polman and H. A. Atwater, *Nat. Mater.*, 2010, **9**, 407.

67 H. Tao, N. I. Landy, C. M. Bingham, X. Zhang, R. D. Averitt and W. J. Padilla, *Opt. Express*, 2008, **16**, 7181–7188.

68 K. Sun, P. Xie, Z. Wang, T. Su, Q. Shao, J. Ryu, X. Zhang, J. Guo, A. Shankar and J. Li, *Polymer*, 2017, **125**, 50–57.

69 H. Chen, L. Ran, J. Huangfu, X. Zhang, K. Chen, T. M. Grzegorczyk and J. A. Kong, *Phys. Rev. E: Stat., Nonlinear, Soft Matter Phys.*, 2004, **70**, 057605.

70 R. Lopez-Martens, K. Varjú, P. Johnsson, J. Mauritsson, Y. Mairesse, P. Salieres, M. B. Gaarde, K. J. Schafer, A. Persson and S. Svanberg, *Phys. Rev. Lett.*, 2005, **94**, 033001.

71 T. J. Yen, W. Padilla, N. Fang, D. Vier, D. Smith, J. Pendry, D. Basov and X. Zhang, *Science*, 2004, **303**, 1494–1496.

72 M. S. Rill, C. Plet, M. Thiel, I. Staude, G. Von Freymann, S. Linden and M. Wegener, *Nat. Mater.*, 2008, **7**, 543.

73 C. R. Garcia, J. Correa, D. Espalin, J. H. Barton, R. C. Rumpf, R. Wicker and V. Gonzalez, *Prog. Electromagn. Res.*, 2012, **34**, 75–82.

74 H. Li, J. Wang, Z. Pan, L. Cui, L. Xu, R. Wang, Y. Song and L. Jiang, *J. Mater. Chem.*, 2011, **21**, 1730–1735.

75 J. A. Fan, C. Wu, K. Bao, J. Bao, R. Bardhan, N. J. Halas, V. N. Manoharan, P. Nordlander, G. Shvets and F. Capasso, *Science*, 2010, **328**, 1135–1138.

76 D. R. Smith, W. J. Padilla, D. Vier, S. C. Nemat-Nasser and S. Schultz, *Phys. Rev. Lett.*, 2000, **84**, 4184.

77 K. Fan, A. C. Strikwerda, H. Tao, X. Zhang and R. D. Averitt, *Opt. Express*, 2011, **19**, 12619–12627.

78 K. Dietrich, D. Lehr, C. Helgert, A. Tünnermann and E. B. Kley, *Adv. Mater.*, 2012, **24**, 321–325.

79 M. Esposito, V. Tasco, F. Todisco, A. Benedetti, D. Sanvitto and A. Passaseo, *Adv. Opt. Mater.*, 2014, **2**, 154–161.

80 I. W. Moran, A. L. Briseno, S. Loser and K. R. Carter, *Chem. Mater.*, 2008, **20**, 4595–4601.

81 K. Nomura, H. Ohta, A. Takagi, T. Kamiya, M. Hirano and H. Hosono, *Nature*, 2004, **432**, 488–492.

82 Z. M. Dang, T. Zhou, S. H. Yao, J. K. Yuan, J. W. Zha, H. T. Song, J. Y. Li, Q. Chen, W. T. Yang and J. Bai, *Adv. Mater.*, 2009, **21**, 2077–2082.

83 L. Zhu, J. Kapraun, J. Ferrara and C. J. Chang-Hasnain, *Optica*, 2015, **2**, 255–258.

84 J. Henzie, M. H. Lee and T. W. Odom, *Nat. Nanotechnol.*, 2007, **2**, 549–554.

85 S. Zhang, W. Fan, B. Minhas, A. Frauenglass, K. Malloy and S. Brueck, *Phys. Rev. Lett.*, 2005, **94**, 037402.

86 D. Chanda, K. Shigeta, S. Gupta, T. Cain, A. Carlson, A. Mihi, A. J. Baca, G. R. Bogart, P. Braun and J. A. Rogers, *Nat. Nanotechnol.*, 2011, **6**, 402–407.

87 K. Fan, A. C. Strikwerda, X. Zhang and R. D. Averitt, *Phys. Rev. B: Condens. Matter Mater. Phys.*, 2013, **87**, 161104.

88 N. Han, Z. Chen, C. Lim, B. Ng and M. Hong, *Opt. Express*, 2011, **19**, 6990–6998.

89 D. Wu, N. Fang, C. Sun, X. Zhang, W. J. Padilla, D. N. Basov, D. R. Smith and S. Schultz, *Appl. Phys. Lett.*, 2003, **83**, 201–203.

90 W. Fan, B. Yan, Z. Wang and L. Wu, *Sci. Adv.*, 2016, **2**, e1600901.

91 U. Zywietz, A. B. Evlyukhin, C. Reinhardt and B. N. Chichkov, *Nat. Commun.*, 2014, **5**, 3402.

92   P. Moitra, Y. Yang, Z. Anderson, I. I. Kravchenko, D. P. Briggs and J. Valentine, *Nat. Photonics*, 2013, **7**, 791–795.

93   H. Chen, L. Ran, D. Wang, J. Huangfu, Q. Jiang and J. A. Kong, *Appl. Phys. Lett.*, 2006, **88**, 031908.

94   B. Liu, X. Zhao, W. Zhu, W. Luo and X. Cheng, *Adv. Funct. Mater.*, 2008, **18**, 3523–3528.

95   D. A. Pawlak, S. Turczynski, M. Gajc, K. Kolodziejak, R. Diduszko, K. Rozniatowski, J. Smalc and I. Vendik, *Adv. Funct. Mater.*, 2010, **20**, 1116–1124.

96   S. S. Mohammed, K. Ramasamy and T. Shanmuganantham, *Int. J. Comput. Appl.*, 2010, **1**, 100–103.

97   J. Garnica, R. A. Chinga and J. Lin, *Proc. IEEE*, 2013, **101**, 1321–1331.

98   W. C. Brown, *IEEE Trans. Microwave Theory Tech.*, 1984, **32**, 1230–1242.

99   P. E. Glaser, *Science*, 1968, **162**, 857–861.

100 H. Matsumoto, *IEEE Microw. Mag.*, 2002, **3**, 36–45.

101 J. O. McSpadden and J. C. Mankins, *IEEE Microw. Mag.*, 2002, **3**, 46–57.

102 W. C. Brown and E. E. Eves, *IEEE Trans. Microwave Theory Tech.*, 1992, **40**, 1239–1250.

103 K. Huang and X. Zhou, *IComM*, 2015, **53**, 86–93.

104 N. Shimokura, N. Kaya, M. Shinohara and H. Matsumoto, *IEEE Microw. Mag.*, 1997, **120**, 33–39.

105 B. Wang and K. H. Teo, *IEEE*, 2012, 161–164.

106 A. Karalis, J. D. Joannopoulos and M. Soljačić, *Ann. Phys.*, 2008, **323**, 34–48.

107 A. A. Eteng, S. K. A. Rahim, C. Y. Leow, S. Jayaprakasam and B. W. Chew, *Renewable Sustainable Energy Rev.*, 2017, **77**, 486–505.

108 J. Schuder, H. Stephenson and J. Townsend, *Inst. Radio Engrs. Int Conv. Record*, 1961, **9**, 119–126.

109 N. D. N. Donaldson and T. Perkins, *Med. Biol. Eng. Comput.*, 1983, **21**, 612–627.

110 R. E. Hamam, A. Karalis, J. Joannopoulos and M. Soljačić, *Ann. Phys.*, 2009, **324**, 1783–1795.

111 M. Kiani, U. M. Jow and M. Ghovanloo, *IEEE Trans. Circuits Syst.*, 2011, **5**, 579–591.

112 Y. Zhang, Z. Zhao and K. Chen, *IEEE Trans. Ind. Appl.*, 2014, **50**, 2436–2445.

113 Y. Zhang, Z. Zhao and K. Chen, *IEEE Trans. Power Electron.*, 2014, **29**, 1058–1063.

114 H. Hoang, S. Lee, Y. Kim, Y. Choi and F. Bien, *IEEE Trans. Consum. Electron.*, 2012, **58**, 327–332.

115 H. Hwang, J. Moon, B. Lee, C. Jeong and S. Kim, *IEEE Trans. Broadcast Telev. Receivers*, 2014, **60**, 203–209.

116 A. Kurs, A. Karalis, R. Moffatt, J. D. Joannopoulos, P. Fisher and M. Soljačić, *Science*, 2007, **317**, 83–86.

117 J. Park, Y. Tak, Y. Kim, Y. Kim and S. Nam, *IEEE Trans. Antennas Propag.*, 2011, **59**, 1769–1773.

118 T. P. Duong and J. W. Lee, *IEEE Microw. Wireless Compon. Lett.*, 2011, **21**, 442–444.

119 T. C. Beh, M. Kato, T. Imura, S. Oh and Y. Hori, *IEEE Trans. Ind. Electron.*, 2013, **60**, 3689–3698.

120 J. Kim, H. C. Son, K. H. Kim and Y. J. Park, *IEEE Microw. Wirel. Co.*, 2011, **10**, 389–392.

121 F. Zhang, S. A. Hackworth, W. Fu, C. Li, Z. Mao and M. Sun, *IEEE Trans. Magn*, 2011, **47**, 1478–1481.

122 W. S. Lee, W. I. Son, K. S. Oh and J. W. Yu, *IEEE Trans. Ind. Electron.*, 2013, **60**, 350–359.

123 W. S. Lee, H. S. Jang, K. S. Oh and J. W. Yu, *IEEE Trans. Antennas Propag.*, 2013, **61**, 3400–3403.

124 B. C. Park and J. H. Lee, *IEEE Trans. Antennas Propag.*, 2014, **62**, 2851–2856.

125 J. Kim, W.-S. Choi and J. Jeong, *Prog. Electromagn. Res.*, 2013, **138**, 197–209.

126 B. Wang, T. Nishino and K. H. Teo, *IEEE Int. Conf.*, 2010, 1–4.

127 J. Wu, B. Wang, W. S. Yerazunis and K. H. Teo, *IEEE*, 2013, 155–158.

128 A. Ranaweera, C. A. Moscoso and J. W. Lee, *J. Phys. D: Appl. Phys.*, 2015, **48**, 455104.

129 D. Huang, Y. Urzhumov, D. R. Smith, K. Hoo Teo and J. Zhang, *J. Appl. Phys.*, 2012, **111**, 064902.

130 Y. Urzhumov and D. R. Smith, *Phys. Rev. B: Condens. Matter Mater. Phys.*, 2011, **83**, 205114.

131 B. Wang, D. Ellstein and K. H. Teo, *IEEE*, 2012, 964–967.

132 Y. Fan, L. Li, S. Yu, C. Zhu and C. H. Liang, *Prog. Electromagn. Res.*, 2013, **141**, 769–784.

133 Y. Xia and L. Wang, *IEEE*, 2008, 1–3.

134 E. S. G. Rodríguez, A. K. RamRakhyani, D. Schurig and G. Lazzi, *IEEE Trans. Microwave Theory Tech.*, 2016, **64**, 1644–1654.

135 S. Lee, S. Kim and C. Seo, *IEEE*, 2013, 1036–1038.

136 S. H. Kang, J. H. Choi and C. W. Jung, *IEEE Trans. Broadcast Telev. Receivers*, 2015, **61**, 160–166.

137 S. Kim, J. S. Ho and A. S. Poon, *Phys. Rev. Lett.*, 2013, **110**, 203905.

138 S. Kim, J. S. Ho, L. Y. Chen and A. S. Poon, *Appl. Phys. Lett.*, 2012, **101**, 073701.

139 Q. Xu, Z. Gao, H. Wang, J. He, Z.-H. Mao and M. Sun, *IEEE Microw. Mag.*, 2013, **14**, 63–72.

140 Q. Wu, Y. Li, N. Gao, F. Yang, Y. Chen, K. Fang, Y. Zhang and H. Chen, *Europhys. Lett.*, 2015, **109**, 68005.

141 L. Zhu, X. Luo and H. Ma, *Appl. Phys. Lett.*, 2016, **109**, 024103.

142 G. Lipworth, J. Ensworth, K. Seetharam, D. Huang, J. S. Lee, P. Schmalenberg, T. Nomura, M. S. Reynolds, D. R. Smith and Y. Urzhumov, *Sci. Rep.*, 2014, **4**, 3642.

143 N. Fang, H. Lee, C. Sun and X. Zhang, *Science*, 2005, **308**, 534–537.

144 R. Merlin, *Science*, 2007, **317**, 927–929.

145 S. Nikoletseas, Y. Yang and A. Georgiadis, *Wireless Power Transfer Algorithms, Technologies and Applications in Ad Hoc Communication Networks*, Springer, 2016.

146 Y. Zhang, H. Tang, C. Yao, Y. Li and S. Xiao, *AIP Adv.*, 2015, **5**, 017142.

147 A. Ranaweera, T. P. Duong, B. S. Lee and J. W. Lee, *IEEE*, 2014, 92–95.

148 J. Choi and C. Seo, *Prog. Electromagn. Res.*, 2010, **106**, 33–47.

149 A. Ranaweera, T. P. Duong and J. W. Lee, *J. Appl. Phys.*, 2014, **116**, 043914.

150 T. Oh and B. Lee, *J. Electromagn. Eng. Sci.*, 2013, **13**, 259–262.

151 A. Rajagopalan, A. K. Ram Rakhyani, D. Schurig and G. Lazzi, *IEEE Trans. Microwave Theory Tech.*, 2014, **62**, 947–955.

152 A. Alphones and J. Sampath, *IEEE*, 2015, 1–3.

153 T. Tsutaoka, T. Kasagi, S. Yamamoto and K. Hatakeyama, *J. Magn. Magn. Mater.*, 2015, **383**, 139–143.

154 K. Sun, R. Fan, Y. Yin, J. Guo, X. F. Li, Y. Lei, L. An, C. Cheng and Z. Guo, *J. Phys. Chem. C*, 2017, **121**, 7564–7571.

155 Z. Shi, R. Fan, Z. Zhang, K. Yan, X. Zhang, K. Sun, X. Liu and C. Wang, *J. Mater. Chem. C*, 2013, **1**, 1633–1637.

156 Z. Shi, R. Fan, K. Yan, K. Sun, M. Zhang, C. Wang, X. Liu and X. Zhang, *Adv. Funct. Mater.*, 2013, **23**, 4123–4132.

157 (*a*) J. Zhu, S. Wei, L. Zhang, Y. Mao, J. Ryu, P. Mavinakuli, A. B. Karki, D. P. Young and Z. Guo, *J. Phys. Chem. C*, 2010, **114**, 16335–16342; (*b*) H. Wu, Y. Zhang, R. Yin, W. Zhao, X. Li and L. Qian, *Adv. Compos. Hybrid Mater.*, 2018, **1**, 168–176; (*c*) J. Zhao, L. Wu, C. Zhan, Q. Shao, Z. Guo and L. Zhang, *Polymer*, 2017, **133**, 272–287; (*d*) Z. Hu, Q. Shao, Y. Huang, L. Yu, D. Zhang, X. Xu, J. Lin, H. Liu and Z. Guo, *Nanotechnology*, 2018, DOI: 10.1088/1361-6528/aab010; (*e*) F. Luo, X. Liu, C. Shao, J. Zhang, C. Shen and Z. Guo, *Mater. Des.*, 2018, **144**, 25–31; (*f*) Z. Hu, D. Zhang, L. Yu

and Y. Huang, *J. Mater. Chem. B*, 2018, **6**, 518–526; (*g*) Z. Hu, C. Wang and F. Zhao, *et al.*, *Nanoscale*, 2017, **9**, 8825; (*h*) Y. Li, B. Zhou, G. Zheng, X. Liu, T. Li, C. Yan, C. Cheng, K. Dai, C. Liu, C. Shen and Z. Guo, *J. Mater. Chem. C*, 2018, **6**, 2258–2269; (*i*) Z. Wu, S. Gao, L. Chen, D. Jiang, Q. Shao, B. Zhang, Z. Zhai, C. Wang, M. Zhao, Y. Ma, X. Zhang, L. Weng, M. Zhang and Z. Guo, *Macromol. Chem. Phys.*, 2017, **218**, 1700357.

158 R. Yin, H. Wu, K. Sun, X. Li, C. Yan, W. Zhao, Z. Guo and L. Qian, *J. Phys. Chem. C*, 2018, **122**, 1791–1799.

159 (*a*) P. Xie, Z. Wang, K. Sun, C. Cheng, Y. Liu and R. Fan, *Appl. Phys. Lett.*, 2017, **111**, 112903; (*b*) H. Gu, C. Liu, J. Zhu, J. Gu, E. K. Wujcik, L. Shao, N. Wang, H. Wei, R. Scaffaro, J. Zhang and Z. Guo, *Adv. Compo. Hybrid Mater.*, 2018, **1**, 1–5.

160 Z. Wang, K. Sun, P. Xie, Y. Liu and R. Fan, *J. Phys.: Condens. Matter*, 2017, **29**, 365703.

161 C. Cheng, R. Fan, Z. Wang, Q. Shao, X. Guo, P. Xie, Y. Yin, Y. Zhang, L. An, Y. Lei, J. E. Ryu, A. Shankar and Z. Guo, *Carbon*, 2017, **125**, 103–112.

162 H. Liu, Y. Li, K. Dai, G. Zheng, C. Liu, C. Shen, X. Yan, J. Guo and Z. Guo, *J. Mater. Chem. C*, 2016, **4**, 157–166.

163 Z. Shi, J. Wang, F. Mao, C. Yang, C. Zhang and R. Fan, *J. Mater. Chem. A*, 2017, **5**, 14575–14582.

This journal is © The Royal Society of Chemistry 2018

J. Mater. Chem. C, 2018, **6**, 2925–2943 | **2943**